Develop a Low Cost, Safe and Environmentally Benign High Energy and High Rate Reserve Battery

SERDP Project Number: 1360
MaxPower, Inc.
David Chua
September 30, 2004
Original Version

Report Documentation Page

Form Approved
OMB No. 0704-0188

1. REPORT DATE	2. REPORT TYPE	3. DATES COVERED
30 SEP 2004	**Final**	**-**

4. TITLE AND SUBTITLE	5a. CONTRACT NUMBER
Develop a Low Cost, Safe and Environmentally Benign High Energy and High Rate Reserve Battery	5b. GRANT NUMBER
	5c. PROGRAM ELEMENT NUMBER
6. AUTHOR(S) **David Chua**	5d. PROJECT NUMBER **PP 1360**
	5e. TASK NUMBER
	5f. WORK UNIT NUMBER
7. PERFORMING ORGANIZATION NAME(S) AND ADDRESS(ES) **MaxPower, Inc. 141 Christopher Lane Harleysville PA 19438**	8. PERFORMING ORGANIZATION REPORT NUMBER
9. SPONSORING/MONITORING AGENCY NAME(S) AND ADDRESS(ES) **Strategic Environmental Research & Development Program 901 N Stuart Street, Suite 303 Arlington, VA 22203**	10. SPONSOR/MONITOR'S ACRONYM(S) **SERDP**
	11. SPONSOR/MONITOR'S REPORT NUMBER(S)

12. DISTRIBUTION/AVAILABILITY STATEMENT
Approved for public release, distribution unlimited

13. SUPPLEMENTARY NOTES
The original document contains color images.

14. ABSTRACT

15. SUBJECT TERMS

16. SECURITY CLASSIFICATION OF:			17. LIMITATION OF ABSTRACT	18. NUMBER OF PAGES	19a. NAME OF RESPONSIBLE PERSON
a. REPORT **unclassified**	b. ABSTRACT **unclassified**	c. THIS PAGE **unclassified**	**UU**	**49**	

Standard Form 298 (Rev. 8-98)
Prescribed by ANSI Std Z39-18

CLEARANCE REQUEST FOR PUBLIC RELEASE OF DEPARTMENT OF DEFENSE INFORMATION

(See Instructions on back.)

(This form is to be used in requesting review and clearance of DoD information proposed for public release in accordance with DoDD 5230.9.)

TO: Director, Freedom of Information & Security Review, Rm. 2C757, Pentagon

1. DOCUMENT DESCRIPTION

a. TYPE	b. TITLE
Final Report	Develop a Low Cost, Safe and Environmentally Benign High Energy and High Rate Reserve Battery (PP-1360)
c. PAGE COUNT: 48	d. SUBJECT AREA: Strategic Environmental Research & Development Program (SERDP)

2. AUTHOR/SPEAKER

a. NAME *(Last, First, Middle Initial)*	b. RANK	c. TITLE
David Chua		
d. OFFICE: Max Power Inc.		e. AGENCY: Max Power Inc., Harleysville, PA

3. PRESENTATION/PUBLICATION DATA *(Date, Place, Event)*

Posting on the SERDP web site.

CLEARED
For Open Publication

MAR 18 2005

Office of Freedom of Information
and Security Review
Department of Defense

4. POINT OF CONTACT

a. NAME *(Last, First, Middle Initial)*	b. TELEPHONE NO. *(Include Area Code)*
Kelly, Amy	703-579-8052

5. PRIOR COORDINATION

a. NAME *(Last, First, Middle Initial)*	b. OFFICE/AGENCY	c. TELEPHONE NO. *(Include Area Code)*
Smith, Bradley	SERDP Executive Director	703-696-2121
Pellerin, Charles	SERDP Pollution Prevention Program Manager	703-696-2128

6. REMARKS

THE INFORMATION CONTAINED IN THIS REPORT FALLS UNDER THE PURVIEW OF THIS OFFICE.

WHEN CLEARED, PLEASE FAX DD-1910 TO 703-478-0526. ATTN: Lucia Valentino (phone: 703-736-4549)

if mailed: 1155 Herndon Parkway, Suite 900, Herndon, VA 20170

7. RECOMMENDATION OF SUBMITTING OFFICE/AGENCY

a. THE ATTACHED MATERIAL HAS DEPARTMENT/OFFICE/AGENCY APPROVAL FOR PUBLIC RELEASE *(qualifications, if any, are indicated in Remarks section)* AND CLEARANCE FOR OPEN PUBLICATION IS RECOMMENDED UNDER PROVISIONS OF DODD 5320.9. I AM AUTHORIZED TO MAKE THIS RECOMMENDATION FOR RELEASE ON BEHALF OF:

Strategic Environmental Research & Development Program

b. CLEARANCE IS REQUESTED BY 20050317 *(YYYYMMDD)*.

c. NAME *(Last, First, Middle Initial)*	d. TITLE
Smith, Bradley P.	Executive Director, Strategic Environmental R&D Program
e. OFFICE: SERDP	f. AGENCY: USD (AT&L)
g. SIGNATURE	h. DATE SIGNED *(YYYYMMDD)*: 20050303

DD FORM 1910, MAR 1998 (EG) PREVIOUS EDITION MAY BE USED. WHS/DIOR, Mar 98

05-S-0958

Front Matter

Table of Contents

Acronyms

PAN	Polyacrylonitrile
$BMIPF_6$	1-Butyl-3-Methylimidazolium hexafluorophosphate
BMItrif	1-Butyl-3-Methylimidazolium trifluoromethanesulfonate
EC	Ethylene carbonate
EMC	Ethyl methyl carbonate
DEC	Diethyl carbonate
DMC	Dimethyl cabonate
γ-BL	γ-butyrolactone
DMSO	Dimethyl sulfoxide
DBP	Dibutyl phthalate
NMP	1-methyl-2-pyrrolindanone
PVdF	Polyvinylidene fluoride
PVdF-HFP	Polyvinylidene fluoride-hexafluoropropylene
PI	Polyimide
XRD	X-ray diffraction

Figures

Tables

Acknowledgements

The accomplishments of this project would be difficult without the contribution and dedication from MaxPower's Principal Development Engineer, Frank Cassel. To a large extent, Mr. Cassel implements and executes almost all the designs of experiments conducted under this program. His contribution in the science and technology of ionic liquid, a new field in lithium-based batteries, merits special recognition. The contribution of Dr. Mark Salomon with respect to the understanding in the field of solute-solvent, and solvent-solvent interactions is also acknowledged.

Executive Summary

Oxyhalide-based primary reserve batteries have been the technology of choice for most of the fuse batteries including the larger reserve batteries for strategic and tactical applications. In particular, the anode is typically metallic lithium, and the cathode depolarizer is, most commonly, thionyl chloride ($SOCl_2$) or sulfuryl chloride (SO_2Cl_2), the latter depolarizer being favored when higher operating voltages are required. Modifications of these oxychloride systems are also being used; for example, the acidification of the electrolyte solutions with $AlCl_3$ for power enhancement and improving activation time. Common to these technologies, however, have been the ever-present issues of safety associated with metallic lithium, of environment and, for that matter, of compatibility with the surrounding equipment. Even a slight presence of moisture could cause corrosion on the surrounding facility overnight and the generation of toxic hydrochloric acid gas with its highly unfavorable impact on the environment.

MaxPower, Inc., has explored the possibility of the Mg/metal oxide system as a possible environmentally friendly and safe alternative to the lithium oxyhalide system. The program was developed to replace the metallic lithium anode with the high energy density material magnesium and replace the oxychloride depolarizer with a high-voltage, high-capacity cathode material such as λ-MnO_2 or MoO_3. The combination of these materials would ideally need an organic solution to support the possible voltage window and achieve the highest energy possible.

The main drawback to the magnesium electrochemical cell is the magnesium anode itself. It tends to form a strong passive oxide layer on its surface that interferes or even prevents electrochemical reactions from occurring. Because of this issue, a large effort was put towards developing methods of removing this film and keeping it from reforming chemically.

With this passive layer, the system voltage upon discharge would be lower than expected. Typically, this is the voltage delay phenomenon exhibited by the anodic passivation film. In anticipation of this issue, we explored designs that would give us the highest battery voltage. We quickly determined that a bipolar cell stack in which the cathode of one cell was connected electrically to the next through a shared substrate would be the best candidate. In this case, the thinner the electrodes, the better the situation was.

The program was broken down into two major tasks. These tasks address issues of the cathode and the anode separately. Once the major characteristics of the system had been determined, the electrodes was examined in terms of a full cell.

The cathode issues are addressed in terms of cathode production methods, process optimization and stability in electrolyte solutions. The great majority of the work is focused on λ-MnO_2. This cathode material was of great interest because of its high voltage versus lithium. Because of our experience with this material in lithium cells, this cathode technology is used as a benchmark to examine processing and electrode modifications for the material itself. Once we were comfortable with its performance in the form that we would have to employ for military applications, we were able to transfer it to the magnesium cell and evaluate the anode. We also assumed that most of the processing knowledge gained through producing thin electrodes with this material could be transferred to other materials.

The anode issues were addressed in terms of alloying materials and stability in electrolyte solutions. The alloying materials were selected and tested based on availability and previous utility in magnesium cells. Focus was placed on one alloy, AZ31B, because it had been used previously in ammonia-based magnesium cells and because of its availability in sheet form. For bipolar stacks, and even for the cells produced for testing, this material was ideal. This material was used to test the stability of the electrolytes and their ability to work with the magnesium without forming an impervious passive film.

Our work in this area quickly produced positive results for the cathode. We were able to produce multiple types of metal oxide cathodes using film deposition method that not only produces thin films, but also can produce highly porous films. When the electrodes are first made, they contain a plasticizer which is subsequently removed to produce a porosity which can then be filled with electrolyte. This success allows us to address the issue of thin films in our battery design.

The anode, on the other hand, presented the greatest challenge. The magnesium oxide layer forms quickly in air, and many of the electrolyte compositions were not able to break down the oxide layer sufficiently enough to produce the optimal system results. In the end, we were forced into removing the oxide layer under an inert atmosphere. This processing step demonstrates the one major challenge remaining in this technology. Having to complete the assembly of a battery under an inert gas in large volumes will increase the cost of producing such a battery.

With the proper processing techniques, we at MaxPower, Inc., were able to produce a cell with a reasonable capacity that could be used to determine a bipolar battery energy. The highest energy ended up coming from the MoO_3 cathode, which ideally in a bipolar stack with 0.05 mm thick Mg plates could produce 9.8 Wh in a D-cell arrangement. This number is lower than a D-cell lithium oxychloride cell, but high enough that it can be used for certain military applications as an adequate replacement for the lithium oxychloride cell. Even though the battery could not replace the entire fleet of lithium-oxychloride batteries and cells, a partial replacement would still lead to an overall decrease in the environmental burden caused by the used of this system.

Objective

The objective of this program is to develop a low cost, safe and environmentally benign high energy and high rate reserve battery such as used in fuses and air-bursting warheads which are equivalent in energy density to that of the presently used metallic lithium - oxychloride reserve battery. To achieve this overall objective, this phase of the program investigates a new reserve battery in which the negative electrode is a magnesium-based material, and the positive electrodes are high voltage, high capacity cathode materials such as λ-MnO_2 (lambda-MnO_2) or MoO_3. This initial effort aims to demonstrate the feasibility of this new reserve cell system under lower rate discharge conditions and to lay the ground work to resolve the challenging issues of anodic passivation that is inherent with magnesium anode.

Background

The active components of the reserve batteries presently used by the U.S. military are classified as hazardous since they contain materials which cannot be disposed in landfills without expensive pretreatment to render them benign, materials which are subject to severe fire hazard, materials which are toxic and produce toxic gases when released into the atmosphere, and materials which are highly corrosive which requires expensive manufacturing processes to insure stability during long term storage. The development of an environmentally friendly and safe reserve battery requires a system which will maintain compliance with relevant environmental statures, regulations and executive orders. The Mg/metal oxide reserve battery originally proposed by MaxPower was anticipated to meet just these requirements.

The majority of the work in the program was performed using λ-MnO_2, a material we have had experience and success with in the past. Our synthesis technique for λ-MnO_2 was developed under a Phase II award to MaxPower by the Army Research Laboratory.[1] Briefly, λ-MnO_2 can be synthesized either by the electrochemical de-lithiation of the spinel $Li_2Mn_2O_4$ or by an acid-wash method. Both techniques delivered an equivalent specific cathode capacity (220 mAh/g) and equivalent rate capability. The rigidity of the spinel structure permits the use of acid leaching and still retained the original spinel structure. This phenomenon is fundamental to the creation of λ-MnO_2 and its associated electrochemical characteristics. After the acid wash, the material typically has a mean particle size of around 10μ and the performance display of this material as a 4.0 volt and 2.8 volt two-plateau cathode is very reproducible. Another reproducibility is the lesser rate sensitivity of the 4.0-volt plateau and it is this finding that permits the proposition of this cathode technology for this battery application, beside the fact that it is an environmentally friendly material. The rate capability of MaxPower's λ-MnO_2 material is excellent as shown in Fig. 1 below, but its rate capability can be increased by using nanometer size material.

[1] US Army Contract DAAL01-97-C-0153

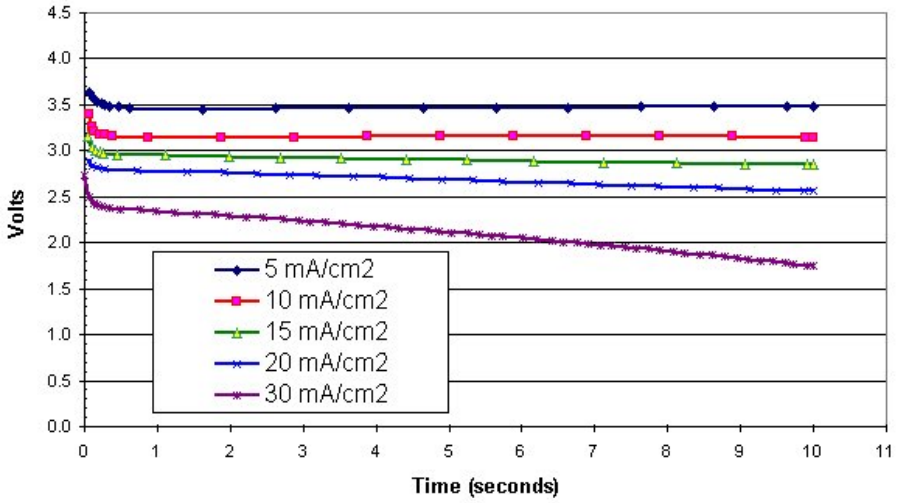

Figure 1: Demonstration of discharge rate capability of λ-MnO_2 cathode in a nonaqueous electrolyte solution corresponding to electronic fuse power demand

Other metal oxides have been explored by other groups in both aqueous and nonaqueous environments. Novák et al reviewed many of the materials explored in this project as possible lithium and magnesium intercalation materials.[2] They found limited information about λ-MnO2, but did note that both the manganese and molybdenum oxides were possible candidates for magnesium intercalation. Kumagai et al explored the hydrated todorokite-type manganese oxide as a possible cathode for magnesium in a non-aqueous environment and met with limited success.[3] Vuorilehto determined that MnO_2 is an acceptable cathode for aqueous magnesium batteries.[4] Aqueous magnesium batteries are discussed extensively in the Handbook of Batteries.[5] We took many of this literature into account when selecting and testing our materials.

Materials and Methods

1. Cathode

Cathode materials were selected based on materials suggested in the literature, their ability to intercalate lithium at high voltages, their probability of intercalating magnesium or their probability of alloying with magnesium. Most of the work was focused on manganese oxides because of their favorable voltage versus lithium, especially in the lambda form. The other material that received more attention because of its favorable results in the literature is MoO_3. We were in possession of a submicron MoO_3 powder that we thought might facilitate the cathode reaction. We also looked briefly into sulfides and carbides to see if the voltage and intercalation capacities warranted further study. Of these materials, only the λ-MnO_2 had to be synthesized.

[2] Petr Novák, Roman Imhof, Otto Haas, *Electrochimica Acta* **45** (1999) 351-367
[3] Naoaki Kumagai, Shinichi Komaba, Hiroiki Sakai, Nobuko Kumagai, *Journal of Power Sources* **97-98** (2001) 515-517
[4] K.Vuorilehto, *Journal of Applied Electrochemistry* **33** (2003) 15 –21
[5] David Linden, Thomas Reddy, Eds. *Handbook of Batteries, 3rd Ed.*, McGraw-Hill: New York, 2002

1.1. Synthesis

λ-MnO_2 is synthesized using two basic techniques. Both techniques begin with a spinel $LiMn_2O_4$. In the first technique, the material is chemically delithiated using sulfuric acid to extract the lithium. This technique was successfully developed at MaxPower, Inc., for US Army Contract DAAL01-97-C-0153 and will be used as the baseline cathode material. The second technique uses electrochemical methods to extract the lithium from the spinel material. In this method, the spinel is mixed with graphite, which acts as a conductivity enhancement, and pressed into thick cathodes. These cathodes are charged at an estimated 100-hour rate to 4.5 V to remove the lithium from the structure. The material is then washed to remove electrolyte and dried before being placed into a new cell as λ-MnO_2. The cell used in this technique is the one described in Formula [1]. Figure 2 shows the voltage profile as the lithium is being removed from the LiMn2O4 to produce the electrochemically synthesized λ-MnO_2.

Lithium Metal/Nickel Current Collector	Electrolyte/Celgard 2300	$LiMn_2O_4$/Conductive Carbon /Aluminum Current Collector	[1]

The reason for the two synthesis paths is because the acid wash yields a material with entrapped hydrogen. This hydrogen can lead to gassing upon long-term storage or discharge. Removing the acid from the synthesis effectively eliminates the hydrogen. If the electrochemically synthesized material performs at least as well as the acid washed material, then it will have a distinct advantage over the acid washed material.

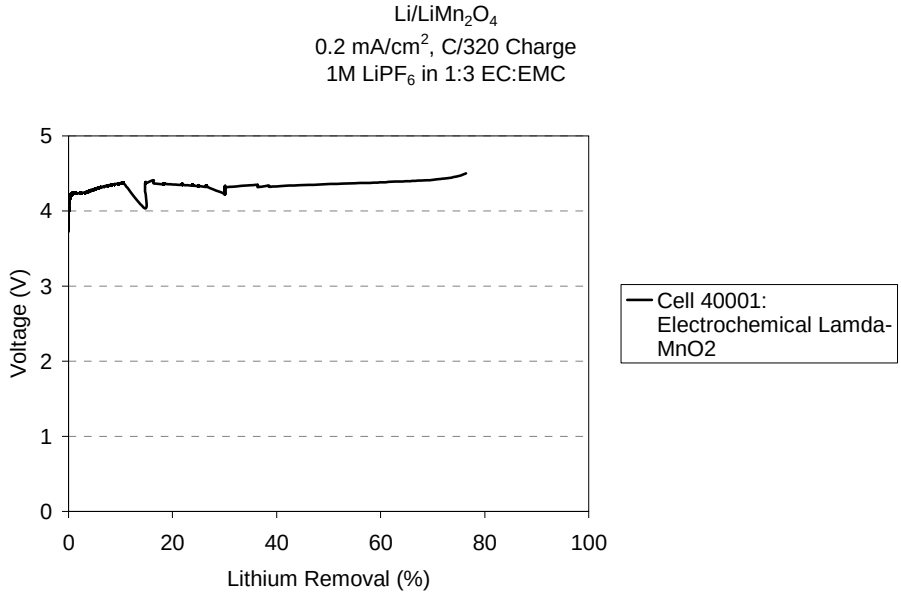

Figure 2: Electrochemical Delithiation Curve for Spinel $LiMn_2O_4$

1.2. Processing

Once the material are produced or received, they must be formed into electrodes. To this end, we have used three processes. One is a thick film process which employs Teflon as a binder and the other two are thin film processes that use PVdF, PVdF-HFP or PI as binders. These

processes were used to determine whether the cathode technology could be transferred from a thick film technology that we had used for this type of cathode before to a thin film technology necessary for the future completion of the battery. These processes are described below.

The vehicle used to test the baseline λ-MnO_2 material is a Teflon pad. The pad is produced through a series of steps. First, the cathode material is mixed with a conductive carbon for several hours. This carbon provides the added electronic connectivity to allow the bulk of the cathode powder to participate in the reaction. This powder mixture is then combined with dry Teflon or Teflon and water and mixed to form the electrode cake. If the Teflon is dry, the mixed powders can be pressed in a die mold to a specific form. If the cake is wet, then it can be rolled onto a substrate, pressed and dried. With this type of technology, the electrode thickness approaches 0.9 mm as a minimum.

With a tape coating process using PVdF or PI homopolymer as the binder instead of Teflon, total thicknesses of 0.1 mm are possible, nearly an order of magnitude thinner than the pressed material. In this process the dry active material and conductive carbon are mixed and then dispersed in a solution of polymer and solvent, NMP. This slurry is then cast onto foil at a certain thickness and dried to form a coating. This coating can be used as is or in a densified form. The cell can be extracted from the coating by cutting a section from it using a die that would allow for a predetermined area of active material and a bare metal lead.

Thicknesses of 0.1 mm can also be achieved by using a lamination-extraction technique with PVdF-HFP. In this process a slurry that contains the cathode material, conductive carbon, polymer binder, a plasticizer and a high vapor pressure solvent is cast onto a glass plate. The solvent, acetone, evaporates leaving behind a film. The film is then laminated onto a metallic substrate and the plasticizer, DBP, extracted, leaving a porous electrode attached to a metal substrate.

When working with λ-MnO_2, we made a point of milling this material to produce a smaller particle size. We were interested in determining whether some advantage could be gained through this exercise in particle size reduction. In this process the material is milled in short periods of one minute or less with a minimum cool down time in between milling periods of at least ten minutes to prevent thermal deterioration of the material. This process is done until a total of fifteen minutes of milling is achieved.

1.3. Characterization

Our two main methods of cathode characterization are X-ray diffraction and electrochemical lithium cells. X-ray diffraction was used primarily to check the lots of λ-MnO_2 for quality and size distribution. The lithium cells were used to determine the effects of the different processing techniques on the performance of the material. This method allowed us to avoid allowing the effects from the magnesium anode to affect our judgment about the cathode processing. This testing was constrained to the λ-MnO_2, as it was our processing model for any other cathode materials might prove to be better than this material, and it was the only material we were to synthesize ourselves.

The X-ray diffraction measurements were done at the University of Pennsylvania's Undergraduate Laboratory. Their facilities include a Rigaku diffractometer, which we can access for powder diffraction testing. The test that we perform at that facility is a 2θ scan from 10° to 80° at 1°/s. The range of this test includes all of the major peaks needed to extract information on the morphology, homogeneity and size of the powder.

Lithium Metal/Nickel Current Collector	Electrolyte/Celgard 2300	λ-MnO_2/Conductive Carbon/Polymer Binder/Aluminum Current Collector	[2]

A lithium cell described by Formula [2] was used to characterize the λ-MnO_2 material in each of two areas: capacity and rate capability. This cell was encapsulated in a laminated bag with an aluminum foil lining to prevent contamination from moisture. The bag was filled and sealed in a glove box with 1M $LiPF_6$ in 1:3 EC:EMC solution as a standard. For the capacity studies, the cell was discharged at 0.1 mA/cm2 until 2 V versus lithium or lower had been reached. This test was the most direct way to determine the condition of the cathode material. For rate capability we have developed a test that incorporates the maximum rates expected in a reserve cell designed based on the thin film technology. In this test, a cell based on Formula [2] using the thin film technology is discharged at either 5 mA/cm2 or 10 mA/cm2 for one minute. If the voltage dropped below 1.6 V before the minute has ended, the test was concluded. For thin electrodes the current should have been some in the range represented by these current densities. This test was used to evaluate the processing techniques and their optimization.

Once tested, these cells can then be disassembled and qualitatively evaluated. Pitting, electrolyte discoloration, uneven lithium usage and gas formation are some of the features that we looked for in disassembling these cells.

2. Anode

The anode materials were selected based mainly on availability and suggestions from the literature for aqueous magnesium batteries. The main materials explored were pure magnesium metal, AZ31B, which is a Mg-Al-Zn alloy with 96% Mg, Mg_2Si and Mg_xC. Of these materials, the AZ31B was the only one which was available in moderate quantities in sheet form. Pure magnesium was purchased as a rod, while the other materials were powders. The only material of this set that we did not purchase was the Mg_xC. This material was synthesized as described below.

2.1. Synthesis

As mentioned above, only the Mg_xC was synthesized in-house at MaxPower. This material was produced by mixing Superior Graphite's synthetic graphite SLA1020 in a beaker with 7N ammonia in methanol. Magnesium ribbon was added to the slurry and allowed to react until the metal disappeared. The ammonia and methanol were then allowed to evaporate and the resulting powder was dried under vacuum at 80°C for 16 hours. With this process we intended to produce an anode material similar to LiC_6, but with magnesium as the intercalated material.

2.2. Processing

Processing is an important step in making the magnesium anode work. The form and reactivity of the anode also played a role in how it could be processed. The powders could only be processed as the cathode powders were in section 1.2 above. The sheet and rod could not undergo such processing, and providing a seal and an electrical connection became an issue.

As far as the powders are concerned, the one that required the greatest amount of attention was the Mg_2Si. This material is moisture sensitive, so any of the slurry-type processes would have been inappropriate, if not dangerous. This material was, therefore, dry-pressed with Teflon as described previously for the cathodes.

Because of the manner in which it was synthesized, the Mg_xC does not need as much care as the Mg_2Si in processing. For that reason, it was produced using the tape casting method described in the section 1.2 above.

The AZ31B electrode is produced by cutting a section from the sheet in the shape that accommodates the cathode shape. The external electrical connection can be made by purely mechanical means or by pressing a nickel grid into the metal using a Sonobond Ultrasonic welder. The oxide layer on the electrode must be removed before being placed in the cell. This removal occurred both under the conditions of either a dry room or an argon-filled glove box.

The magnesium rod or an AZ31B metal strip in certain cases was used with the oxide layer removed in the argon-filled glove box. The connection was made by alligator clip to the end of the rod or strip. The alligator clip was then attached to a wire that could be fed out of the test fixture.

2.3. Characterization

As with the cathode, the characterization of the anode occurred by means of XRD and electrochemical cells. XRD was used mainly to see structural changes from magnesium insertion. The electrochemical testing was used to compare the various anodes and determine the effects of different types of processing.

XRD was used in the anode only for the Mg_xC to determine whether magnesium could at least be detected in the carbon structure, or whether MgO was more prevalent. XRD was also used to determine whether magnesium had been transported to the cathode. All of this testing was done using the same protocol as the cathode described in section 1.3.

The electrochemical testing was modified to fit the magnesium system. The cathodes were used in cells based on Formula [3]. Our initial testing was performed on a system that used a Teflon-bound λ-MnO_2 cathode and a piece of AZ31B or magnesium rod suspended by alligator clips in the electrolyte solution. Figure 3(a) shows a picture of this assembly. This fixture represented our go/no-go test for the system. It was a simple fixture that enabled us to see if an electrochemical reaction was even possible.

Once this characterization was completed, the cell was tested in the more confined fixture shown in Figure 3(b). In this fixture, an AZ31B disk is placed into the bottom of the cylinder shown on

the left. A piece of stainless steel is screwed into the bottom and butted against the magnesium to provide electrical contact. A separator is placed on top of the magnesium to prevent electrical contact, while enabling ionic flow when wetted with the electrolyte. This separator is either a microporous or treated polyethylene both of which wet well in the electrolyte solutions needed for the magnesium cell. A cathode disk is welded to the top connection of the fixture shown in the middle of Figure 3(b). This section provides alignment and allows for the possibility of a reference electrode. The section is inserted into the cylinder shown to the left in Figure 3(b). These two parts are held together in a tight seal by the cap shown to the right in Figure 3(b).

Magnesium-Aluminum Alloy	0.5 M $Mg(ClO_4)_2$ in γ–Butyrolactone	λ-MnO_2/Conductive Carbon/ Polymer Binder/Aluminum Current Collector	[3]

The reasons for moving to the fixture shown in Figure 3(b) are twofold. First, this fixture enables us to seal the cell under a fixed atmosphere. The fixture depicted in Figure 3(a) is difficult to seal, allowing for some transfer of outside atmosphere into the chamber. The fixture shown in Figure 3(b) seals on o-rings at all openings, and therefore allows for substantially reduced atmospheric exchange. Second, a constrained fixture allows us to simulate the conditions of a standard battery type, such as a button cell.


(a) (b)

Figure 3: (a) Open and (b) Constrained Fixtures for Mg/λ-MnO_2 Cell

Eventually, the fixtures in Figure 3(b) began to swell and deform. Not only were they becoming more difficult to reassemble with each use, but they were also beginning to pass the electrolyte from one set of tests onto another set. We, therefore, worked on developing a way to press a nickel grid lead into the magnesium through ultrasonic welding. This metal grid can be used with a heat-sealable bag to protect the cell from the outside atmosphere. This bag has an aluminum lining that prevents any atmospheric exchange. However, for the electrical connection to work, the connector must be brought through the heat seal. The magnesium metal is too thick to be brought through the heat seal, which is why the nickel grid had to be attached to it.

In every case, the cells were discharged at 0.1 mA/cm^2 to 0V versus the anode to determine the full capacity of the system. In certain cases, the voltage was measured versus an AZ31B reference electrode to isolate one or the other electrode. Once the final system was selected, it was tested at the rates described for the lithium-cell rate testing described in section 1.3 above to see if this system could handle these conditions. For this test the 1.6V minimum was removed, as the system has a generally lower voltage than the lithium system.

3. Electrolyte Solution

The electrolyte solutions begin with the electrolyte salt. The electrolyte must contain the Mg^{2+} cation to be most productive. The anions selected were done based on experience from lithium battery electrolytes, availability and the goal to produce an environmentally sound system. The three salts selected were $Mg(ClO_4)_2$, $MgCl_2$ and $Mg(CF_3SO_3)_2$. Of these salts, the perchlorate salt is the least desirable out of safety and environmental concerns and the chloride the most desirable for the same reasons. The perchlorate was used first to test the operation of the magnesium cells, since it had a better chance of going into solution with the aprotic solvents we intended to use than the other two salts. Once the principal system and its trends were determined, we switched to $MgCl_2$.

To begin the electrolyte solution studies, we looked into solvents that could serve as the basis for future investigations. Several criteria were used to select these solvents. The three most important criteria were that they be room temperature liquids, be able to solvate $Mg(ClO_4)_2$ and be stable in the voltage window under consideration. These criteria had to be met for the solvent to be considered for the initial studies. Other criteria were used to determine whether the solvents would be effective in the electrochemical environment. Criteria such as high dielectric constant and low viscosity are necessary traits for the solvent to have success. Also the solvent's miscibility with water was a consideration, as water was in some cases an essential additive in this primarily organic system.

Solvent	Dielectric Constant	Viscosity (cP)	Water Solubility
Propylene Carbonate (PC)	64.92	2.53	Very Soluble
γ-Butyrolactone (γ-BL)	41.77	1.727	Very Soluble
Acetonitrile (AN)	36.64	0.369	Completely Soluble

Table 1: Chemical Properties of Interest for Base Solvents[6]

Three solvents were tested initially based on these criteria. Table 1 summarizes the melting point data and the room temperature dielectric constant and viscosity for the three solvents in question. Each of these solvents is a liquid and is able to solvate to a level of at least 0.5 M $Mg(ClO_4)_2$. MaxPower has had some experience with PC and γ-BL and has found them to be stable with λ-MnO_2. Acetonitrile is attractive because of its low viscosity and high dielectric. Since it has also been used in magnesium cell studies, its stability should not be an issue.[7]

Once a base solvent proved to be promising, we began to improve the qualities of the overall solution with supporting solvents. In choosing supporting solvents to test in the AZ13B/λ-MnO_2 cells, we combined an approach that we felt would help break down the passive layer on the

[6] David R. Lide, Ed. *Handbook of Chemistry and Physics, 75th Ed.* CRC Press: Ann Arbor, 1994.
[7] Petr Novak and Johann Desilvestro, *J. Elelctrochem. Soc.*, **140** (1), 1993, 140

surface of the magnesium with the knowledge we have of lithium metal and lithium ion cell electrolytes. We used the ionic liquid 1-butyl-3-methylimidazolium hexafluorophosphate ($BMIPF_6$) in the solution as one cosolvent. In this capacity the solvent does not detract from the liquid form of the solution itself, and potentially adds to the ionic conductivity through its ionic nature. It also adds to the overall corrosiveness of the solution, which is necessary to break down the passive layer on the magnesium. The one drawback in using ionic liquids is that they can quickly increase the viscosity of the solution. We therefore turned in certain cases to EMC, an organic solvent commonly used in electrolyte solutions for lithium metal and lithium ion electrolytes to lower the overall viscosity of the solution. Finally, DMSO was used specifically with $MgCl_2$. In many solvents, it reaches saturation quickly, at which point, ionic mobility is hindered, making the cells that use these electrolytes less effective. For this material, a solvent that helps enable solubility like DMSO is needed to allow for better ionic mobility.

3.1. Processing

All electrolyte solutions were processed in a similar manner. The salts were typically used as bought, while the solvents were all dried in an argon-filled glove box over molecular sieve for at least 24 hours. The solvents were then mixed in selected mass ratios. The salt was measured to meet a certain molarity for a selected volume. The salt and solvents were combined to produce a solution of the selected molarity.

3.2. Characterization

The characterization of these electrolytes was carried out electrochemically. Conductivity and cell performance were used to compare the solutions. Conductivity is the best measure of the mobility of the ions in solution, while the cells will show the effects of the solvents and electrolytes on the electrode materials.

Conductivity testing was done by immersing platinum probes into the electrolytes solutions and measuring the conductance of the cell and correcting to the conductivity based on the cell constant. This testing was done between -20°C and 60°C to see the effect of temperature on ionic mobility. Other features such as freezing and excessive evaporation of the solvents can be seen with this test procedure. It quickly determines the physical limitations of the solution.

The cell testing was performed on each of the different solutions using the cell described by Formula [3]. The cells were discharged at 0.1 mA/cm^2 to 0 V versus the anode to determine the full capacity of the system. In certain cases, the voltage was measured versus an AZ31B reference electrode to isolate one or the other electrode to see the effect of the electrolyte on one electrode or the other. Once the final system was selected, it was tested at the rates described for the lithium-cell rate testing described in section 1.3 above to see if this system could handle these conditions. For this test the 1.6 V minimum was removed, as the system has a generally lower voltage than the lithium system.

Results and Accomplishments

1. The Cathode System

The cathode system was developed originally on the basis of lithium-MnO_2 cells described by Formula [2]. The initial goal in developing the cathode system was the development of a thin electrode. We, therefore, used the more familiar electrochemical system to evaluate the effects of synthesis paths, electrode processing changes and cell thickness on the cathode. Once the effects were clear, the cells could be used with the intended magnesium anode.

1.1. Synthesis and Characterization of λ-MnO_2 Cathode

The synthesis of the λ-MnO_2 cathode proceeded by two routes. The first is the acid wash method described above. This method is a simple, high-throughput method of producing the λ-MnO_2 material. Some possible disadvantages to this material are its storage capability and gas formation during discharge. Our previous studies suggest that the hydrogen entrapment is a possible factor in the mechanism in both of these cases. The hydrogen comes from the acid wash procedure itself, and to date a method of completely removing the hydrogen from the resultant material has not been devised. We, therefore, explored the second method of electrochemical extraction of $LiMn_2O_4$ to determine whether it was a viable alternative to the chemical extraction.

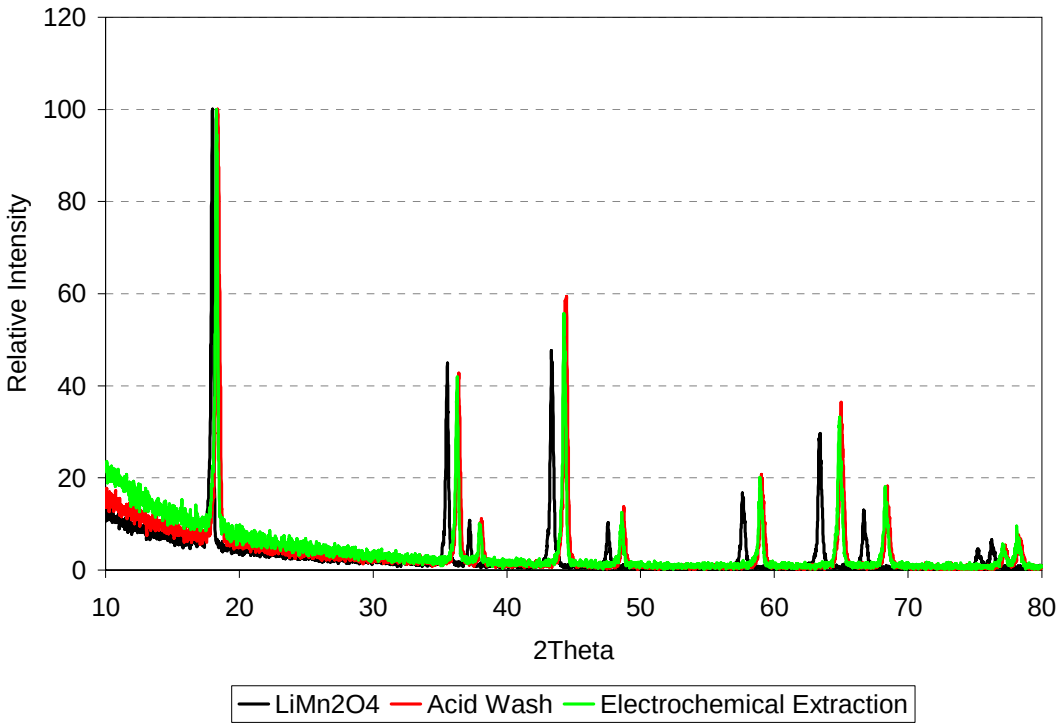

Figure 4: XRD Scan of Precusor $LiMn_2O_4$ and Two Resultant λ-MnO_2 Materials

Figure 4 shows the XRD curves of the source material for each of these methods, $LiMn_2O_4$, and the two resultant materials from each of the synthesis techniques. Since both techniques extract

lithium without changing the actual morphological structure, we expect to see a shift in the XRD peaks representing the shift in size of the lattice structure, but not a rearrangement of the lattice itself. In Figure 4, we see just such a shift. This shift is slightly greater for the acid wash material than the electrochemically extracted material, which is an indication of completeness of the extraction. We expect to see a difference in the discharge characteristics from this XRD scan.

The electrochemical results do reflect this difference in extraction. Figure 5 shows the results of a cell built using a batch of λ-MnO_2 produced for this program. The capacity for the cell using the material produced through chemical extraction demonstrates a better specific capacity than the cell using material produced through electrochemical means. Since the mechanism of the electrochemical reaction is the insertion of lithium, we can conclude that the electrochemical extraction is incomplete by 25%.

This figure also demonstrates several points of interest beginning with the reason why this material has been chosen for this application. Its high voltage plateau at 4 V versus lithium with a similar electrochemical mechanism translates to 3.4 V versus magnesium in the most ideal situation. This plateau produces as much as 120 mAh/g of capacity and is less affected by discharge rate than its second 2.8 V plateau. Even in the electrochemically extracted, although almost a quarter of its original lithium is remaining, cells built from this material still demonstrate the 4 V plateau versus lithium. In fact, most of the loss in capacity due to incomplete delithiation of the spinel material is seen in the 2.8 V plateau, which is of less interest anyway.

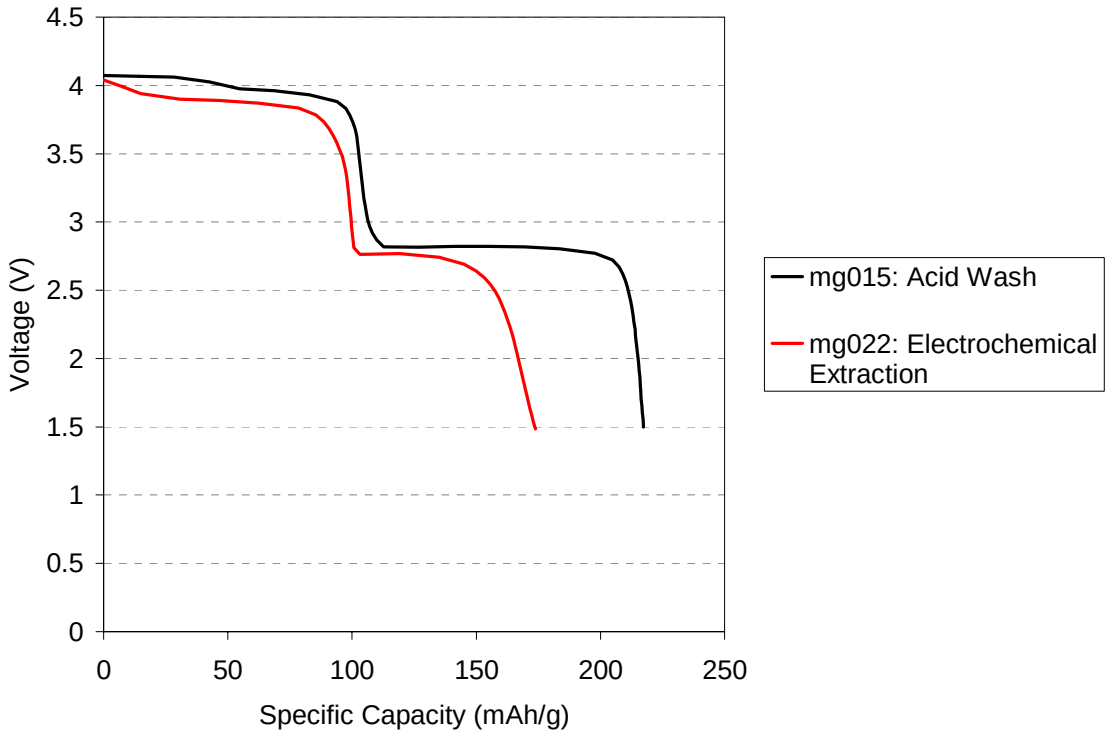

Figure 5: Comparison of Electrochemically and Chemically (Acid Wash) Produced λ-MnO_2

MaxPower has been able to produce two materials for use as high energy, environmentally friendly cathodes for use with magnesium anodes. Since both materials behave similarly and the acid wash represents the most complete lithium extraction and can produce a much larger volume of material, we have focused on this material for processing and testing purposes.

1.2. Processing of the Positive Plate

Film Thickness. In the processing of the positive plate, we have focused on taking this thick-plate technology at 0.9 mm and shrinking it to 0.1 mm. To this end, we explored two alternative processes to the Teflon press technique discussed in the Materials and Methods section. The first and simplest technique is the tape casting technique which deposits the electrode coating directly onto the conductive metal substrate. Once dry, this material can be used immediately as an electrode in the cell. The second technique is the lamination-extraction method, which uses a plasticizer to keep the pore structure in tact while the material is being processed. Once formed to a specific shape, this plasticizer is removed to produce a useable electrode.

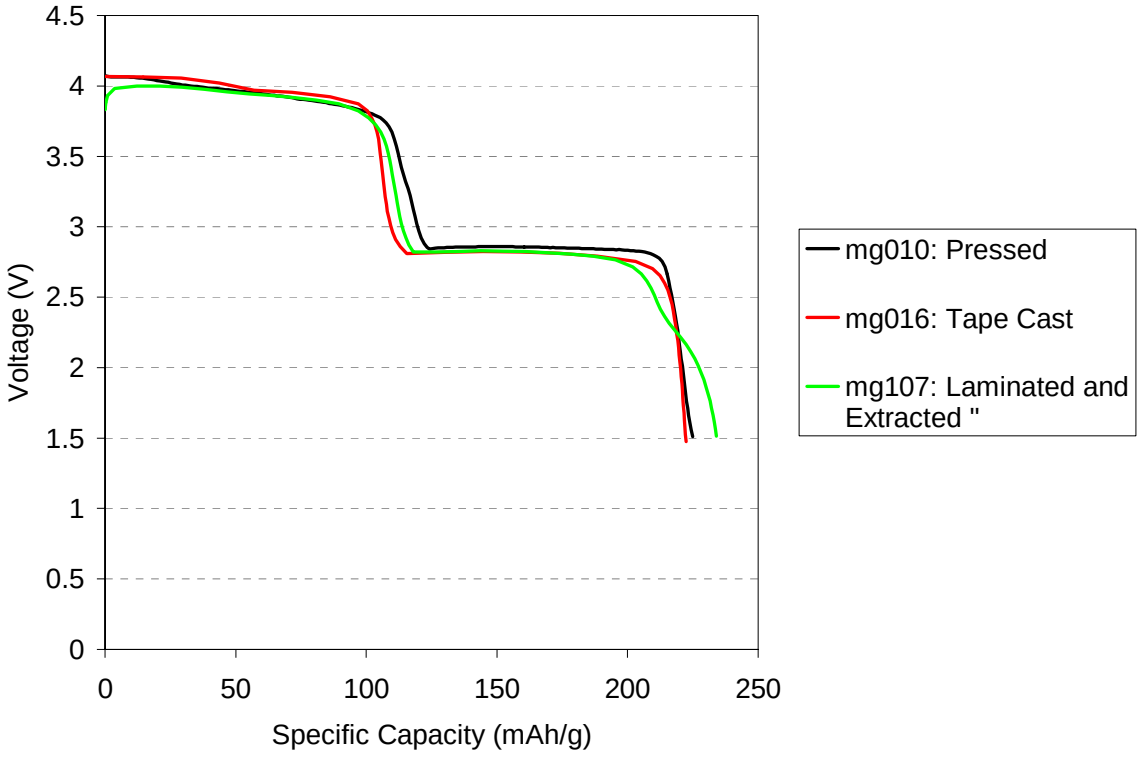

Figure 6: Comparison of λ-MnO_2 Thin Film (PVdF) Cells with Thick Film (PTFE) Baseline

Figure 6 shows the results of a slow discharge of the λ-MnO_2 material from all three electrode processes. These cells were discharged at the same current density, which means that their C-rate discharges are widely divergent. Despite the difference in C-rate, the cells behave similarly, as shown in Figure 6. In general, these coating can be considered baselines for each of the processing techniques because of their similarity to the original Teflon baseline. The only differences are seen in a slight capacity difference in the higher plateau which could be a result of damage to the cathode due to some of the high temperatures seen during the drying of the

NMP for the tape cast material and the lamination for the laminated material. This difference is minimal, and processing cannot be considered a major detriment to the energy delivered.

Ball Milling. Particle size reduction was explored as an option to determine whether the capacity and rate capability of this material could be pushed in a positive direction by increasing the overall available surface area. As a part of this work, the λ-MnO_2 material was ball milled to reduce the particle size. To be successful, this process must not damage the material and should reduce the particle size by at least one order of magnitude.

Figure 7 presents results for the milled and unmilled λ-MnO_2 materials in the tape cast film. The ball milled material shows lower voltages than the baseline material. The transition from one plateau has a lesser slope as well. In general, though, the cell's performance is consistent with the baseline material's performance.

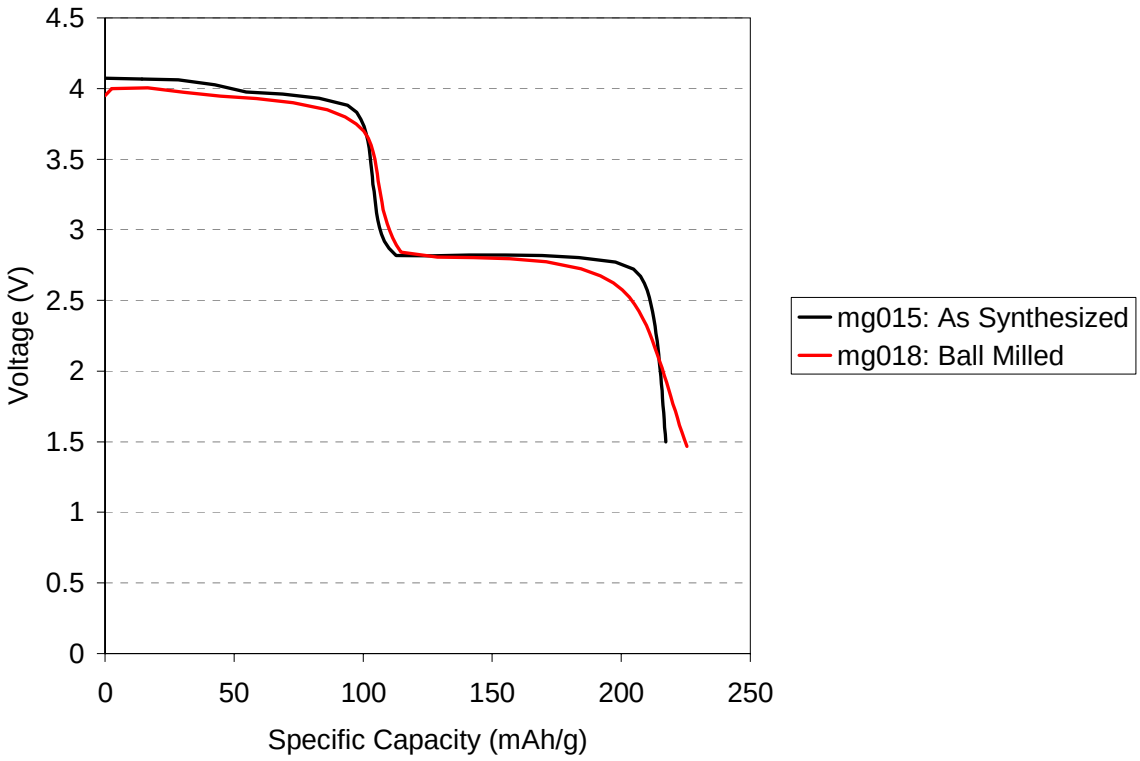

Figure 7: Comparison of Milled and Baseline λ-MnO_2 materials

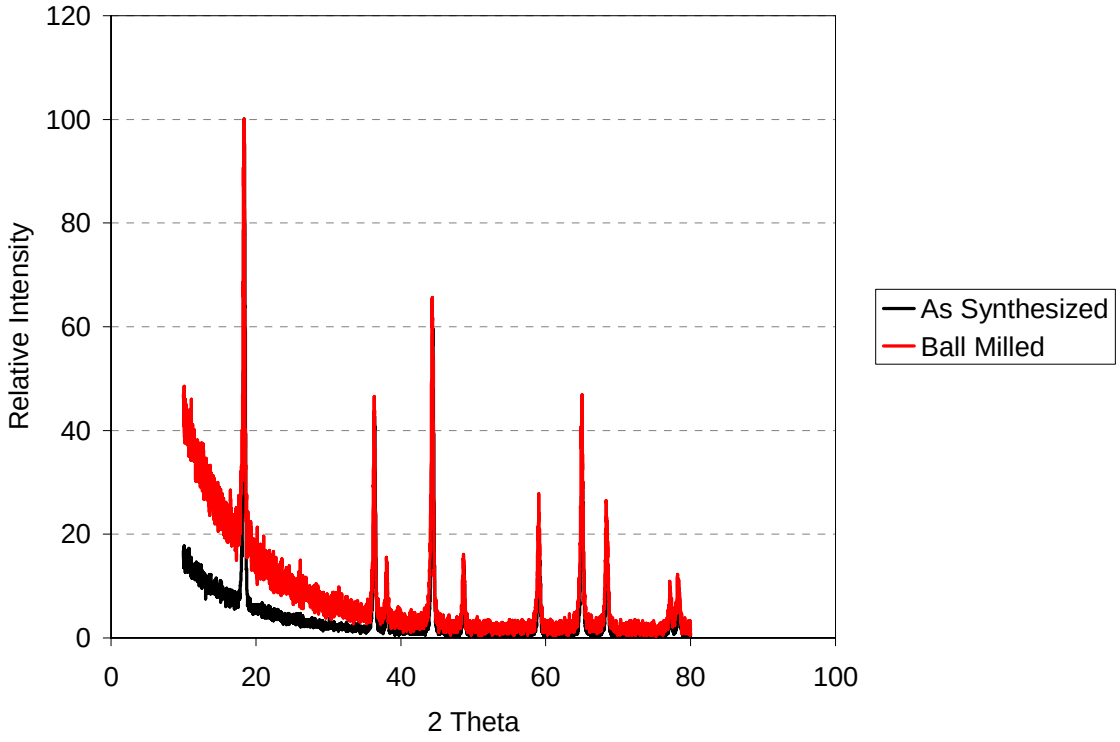

Figure 8: XRD Comparison of Baseline and Ball Milled λ-MnO_2

In addition to electrochemical testing, the effects of ball milling were tested by XRD. Figure 8 shows the results of this testing. For the "As Synthesized" material, the X-ray scan is clear and the peaks are strong, indicating a good degree of crystallinity. The ball milled material, on the other hand, has a less pronounced XRD scan, indicating more amorphous content in the material. The peaks for this material have not moved and have generally the same width indicating that the overall particle size has not changed through this processing.

These materials were then tested at higher discharge rate to determine whether an advantage could be gained by using this more amorphous ball milled material. As an "electronic fuse battery", this type of battery requires a current density of 30 mA/cm^2 for a single-plate cell. If this type of cell is replaced with a thin film multicell configuration, we estimate that the new current density would be between 5 mA/cm^2 and 10 mA/cm^2. This test is described in the Methods and Materials section.

Figure 9 shows the results for both 5 mA/cm^2 and 10 mA/cm^2 for each of the thin film systems discussed above. Figure 9(a) shows the results of the 5 mA/cm^2 while Figure 9(b) shows the results of the cells discharged at 10 mA/cm^2. As far as the performance is concerned, Figure 9(a) shows that at this rate, the two materials are similar in nature. Although the baseline material is somewhat lower in voltage, this drop is not drastic and may have more to do with differences from cell to cell than in the material itself. The high rate does show a more phenomenological response in Figure 9(b). The ball milled material shows a much lower discharge voltage than the

baseline material, indicating that the crystalline baseline is more suited to the high rate application than the amorphous ball milled material.

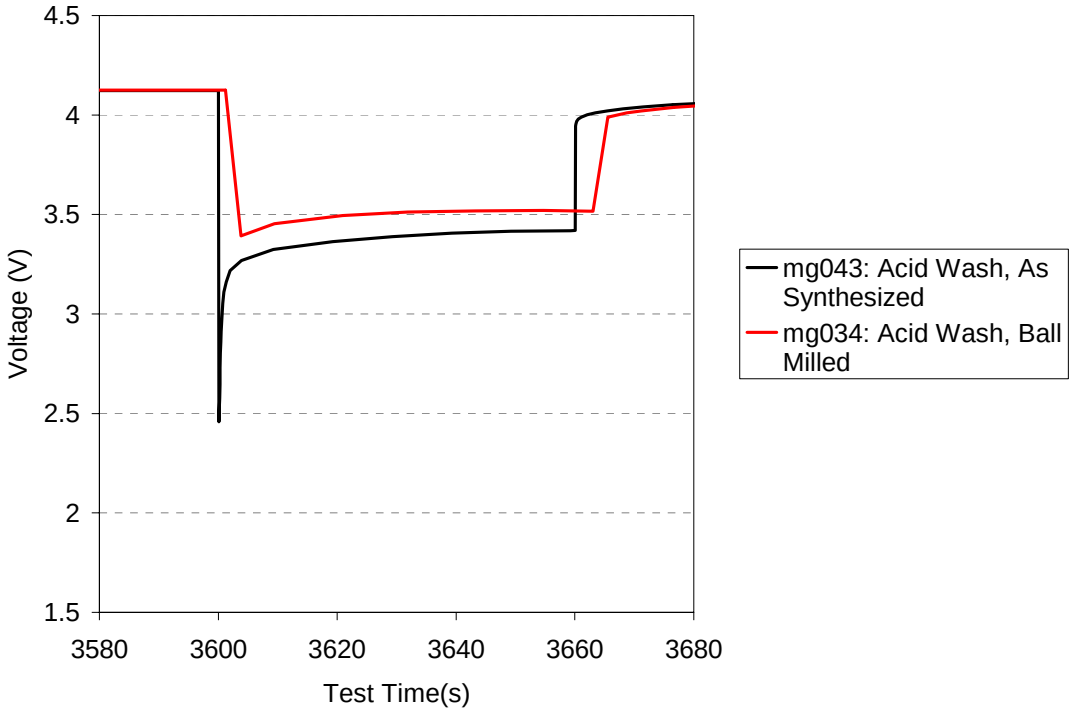

(a)

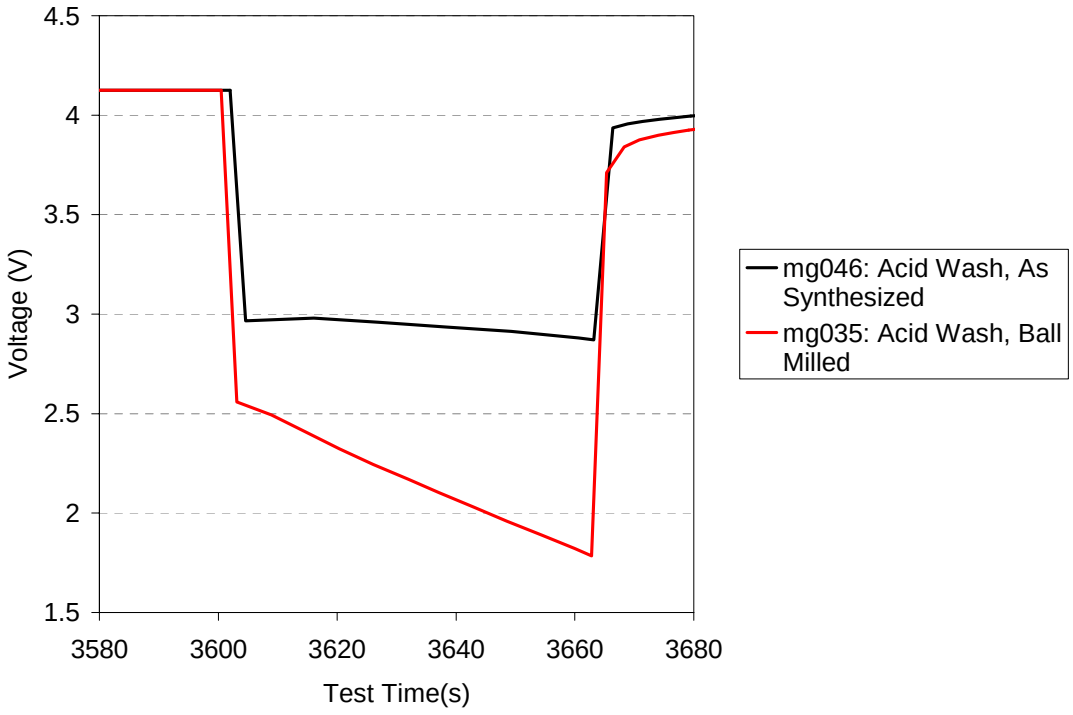

(b)

Figure 9: One Minute Rate Capability of Thin Film (PVdF) Cells at Current Densities of (a) 5 mA/cm^2 and (b) 10 mA/cm^2

The baseline material shows an initial drop in voltage at 5 mA/cm^2 which could be the effect of lithium passivation or of the material itself. This drop is not recorded in the other cell because of the electrochemical test station used to do the testing. In general, when the tester has the resolution to pick up this drop, it is observed in every case. This initial voltage drop is a consideration for "electronic fuse" batteries, because in many cases a minimum activation period must be adhered to in order for the fuse to function properly. This phenomenon was, therefore, tracked in the magnesium cells as an item that would eventually have to be overcome.

1.3. Optimization of the Positive Plates

The focus for the optimization of the positive plates was on the polymers used to bind them to the substrate. PVdF is a standard polymer for lithium and lithium ion cells as a binder for both the cathode and anode because of its stability, despite the fact that its adhesion to metal substrates is fair to poor. When working with thin film technologies, several systems exist that could be used to bind the cathode material to the metal substrate. We focused on three of these thin film systems. Two are familiar from the previous processing section. These systems are the tape cast PVdF system and the laminated-extracted PVdF-HFP system. In addition, we looked at PI, because of its good adhesion to metal substrates. This material was tape cast in the same procedure used for the PVdF cells.

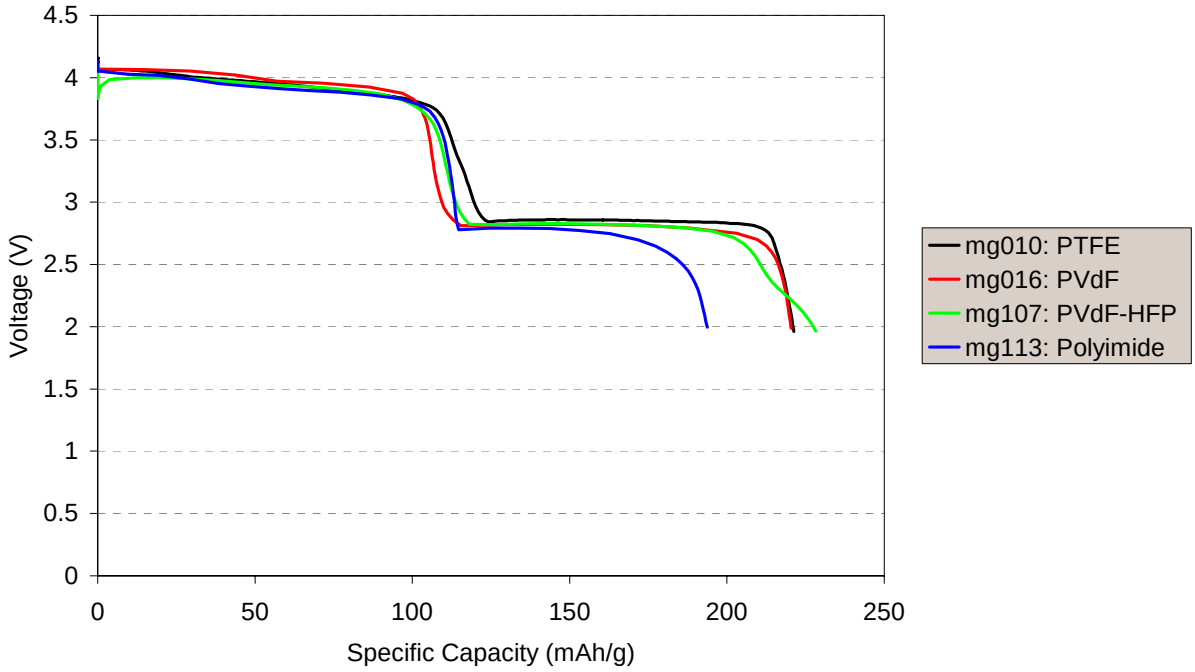

Figure 10: Low Rate Discharge of Li/λ-MnO_2 Cells

Figure 10 illustrates the full discharge profiles of each of the systems under examination. The PTFE system is the baseline system. It demonstrates the major characteristics of the λ-MnO_2 system versus lithium. First, a 4 V plateau is observed which achieves a specific capacity of 120 mAh/g. Then the voltage falls to a second plateau at 2.8 V and discharges until the overall specific capacity is 220 mAh/g.

The other three cells show similar behavior, demonstrating their abilities to support this system to a certain extent. Each system, however, has its advantages and disadvantages. The PVdF tape-cast cathode performed nearly identically to the thicker PTFE cell. Unfortunately, poor adhesion and coat quality make this electrode difficult to handle and process beyond rudimentary assembly. The PVdF-HFP cell was simple to handle and assemble, but it does demonstrate an initial dip in voltage in the discharge and a modified 2.8 V plateau. These features indicate that the λ-MnO_2 material may have received minor damage due to heat conversion during the lamination process. The polyimide cell showed excellent adhesion, but its performance especially in the 2.8 V plateau is not as good as the PTFE cell. Polyimide in high concentrations can impede lithium insertion by covering active intercalation sites. This mechanism may account for the loss in capacity observed.

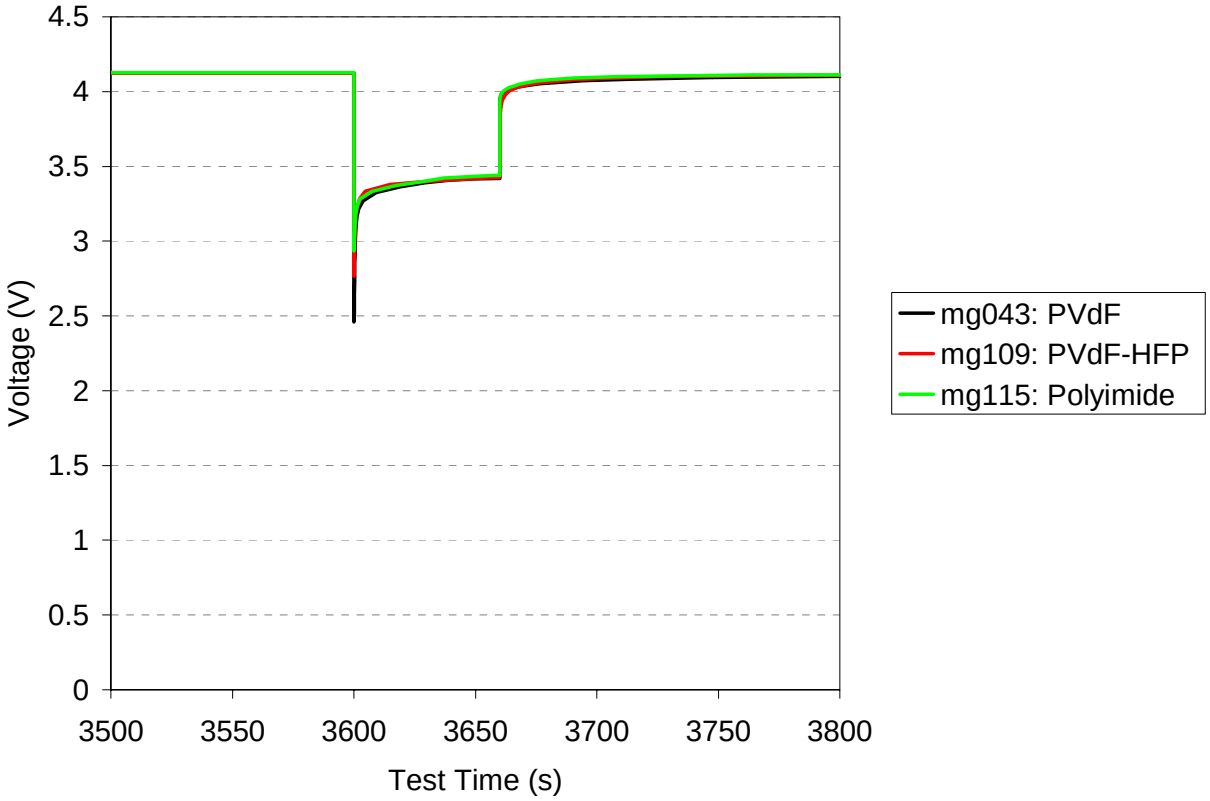

Figure 11

Figure 11: Voltage Profile for 60 Second Discharge at 5 mA/cm^2

A separate issue for these materials is their pulse rate capability. Figure 11 shows the results of a 5 mA/cm^2 discharge current density that lasted for 60 seconds. In this case, the profiles of the three electrode types overlap to a large extent. The main difference is the magnitude of the initial drop in voltage that occurs during the first few seconds of discharge. This difference is highlighted by Figure 12.

This voltage drop may be a capacitive effect from the coating to current collector interface. The amount of polarization seems to be related to the apparent quality of the coating. For the PVdF tape-cast coating the voltage change is the largest of the three. As was stated previously, this coating demonstrates poor adhesion to the current collector making it difficult to handle. The PVdF-HFP laminated coating had a smaller initial voltage drop than the PVdF tape-cast coating, but a larger initial voltage drop than the polyimide coating. Because this coating is laminated to the current collector, the active material contact to the current collector may not be as intimate as that for a coating that is cast directly to the current collector. The polyimide demonstrated the least initial voltage drop. Polyimide films are generally more adhesive than PVdF films, but, as demonstrated previously, do tend to prevent the active material from achieving its full capacity, which is why they are not commonly employed. However, this material is the most effective in limiting the initial potential drop for this cell and for high rate pulse applications, this quality is an advantage.

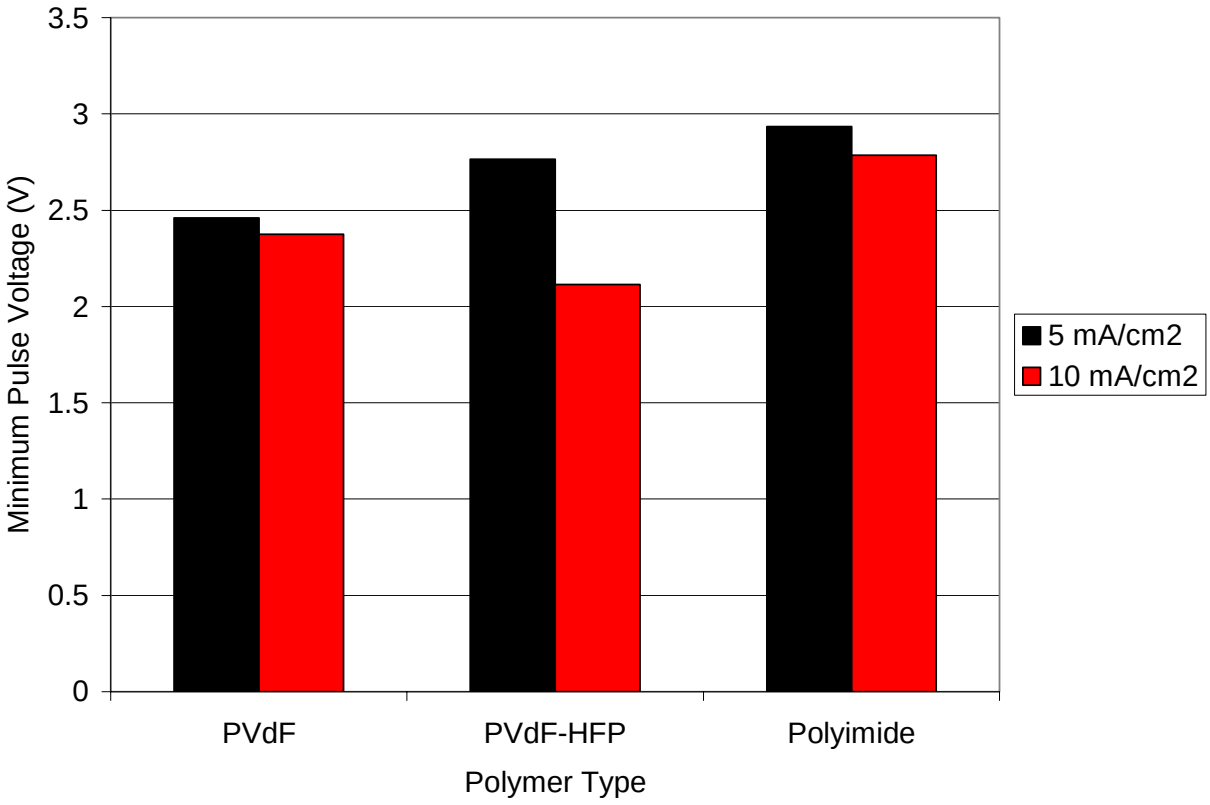

Figure 12

Figure 12: Minimum Voltage for 60 Second Discharge at 5 mA/cm^2

When the 60 second pulse current density is increased to 10 mA/cm^2 as shown in Figure 13, more of a distinction can be made between the three electrode types. Instead of having similar voltage profiles, these profiles now diverge. The polyimide and PVdF tape-cast coatings demonstrate the lower voltage levels, but the polyimide is increasing in voltage with time, while the PVdF voltage is decreasing. The PVdF-HFP demonstrates the best average voltage of these electrodes. It does, however, have a significant initial voltage drop when compared to the

polyimide. As discussed above, this voltage drop seems to be related to the current collector to electrode interface, while the average voltage seems to be related to the availability of the active material itself. With its porous structure and high conductive carbon concentration, the PVdF-HFP electrode has an advantage over the polyimide electrode in the availability of the active material for electrochemical reaction. The PVdF tape-cast coating shows the same initial drop in voltage as the PVdF-HFP, but does not recover as this other system. Despite its shortcomings in the first second or less, the PVdF-HFP seems to hold the advantage over the other two systems. This material demonstrates the open pore structure needed to maximize the intake of magnesium ions.

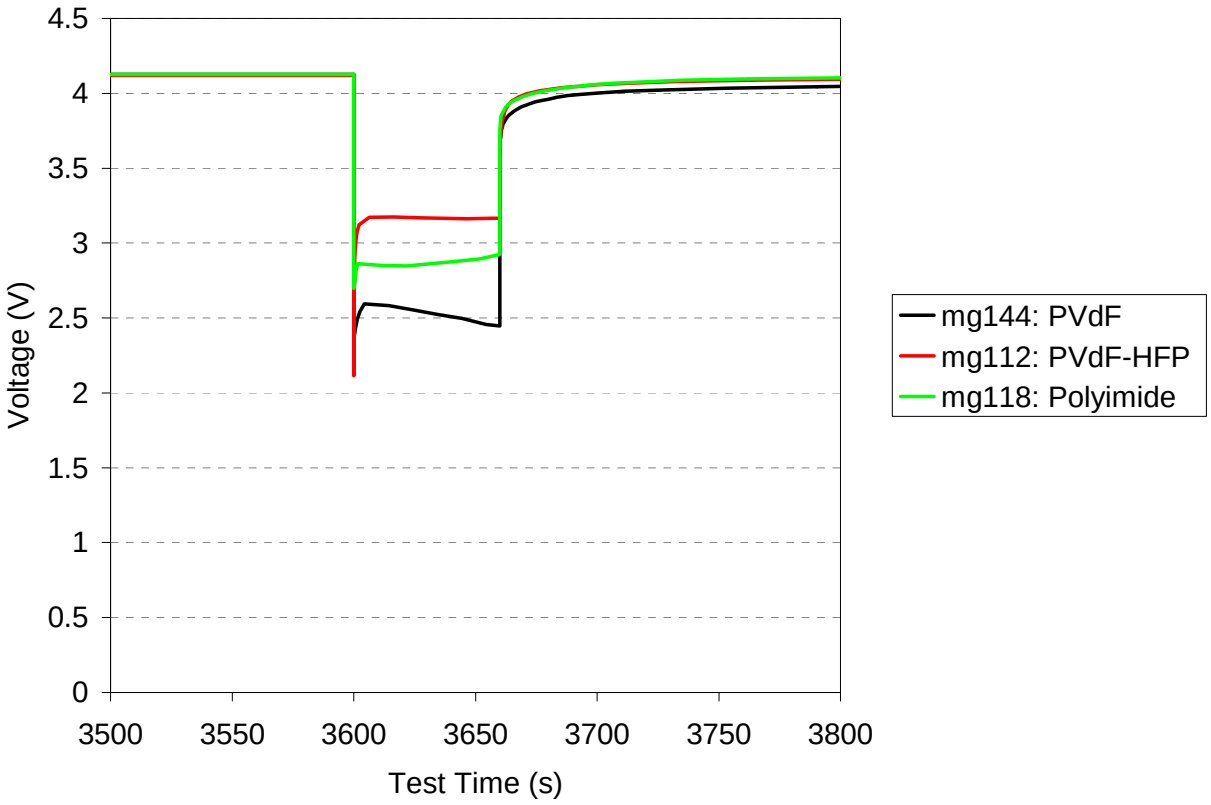

Figure 13: Voltage Profile for 60 Second Discharge at 10 mA/cm^2

2. The Mg Anode System

The magnesium anode has one major challenge that must be overcome before the system can become viable, and that challenge is the oxide layer on its surface. Removing this layer is paramount to the success of the cell. Unlike in a lithium cell, this layer is not conductive, but passive and can effectively remove large portions of the anode from the electrochemical reaction. In this project, MaxPower, Inc. has explored several methods of mitigating this layer. Electrolyte chemistry, low oxide alloys and polishing the anode under inert gases are the three main ways in which we have chosen to deal with this challenge. The effects of these processes will be discussed below in reference to the λ-MnO_2 cathode.

2.1. Optimization of Electrolyte Solution

$Mg(ClO_4)_2$. Magnesium perchlorate was used initially to develop the system of solvents and observe the trends. This salt is readily available, but, as a perchlorate, is not environmentally viable in this type of cell. Once we had established the fundamentals, we moved to exploring environmentally more sound electrolytes such as $MgCl_2$.

In producing an electrolyte solution, we chose the approach that was discussed in the Methods and Materials session when referring to the Table. Much of the work is based on γ-BL, because it had a lower viscosity and higher dielectric constant than PC. In these solutions, we used the ionic liquid 1-butyl-3-methylimidazolium hexafluorophosphate ($BMIPF_6$) in the solution as a corrosive cosolvent to help remove some of the oxide layer on the metal surface and keep it from reforming. In this capacity the solvent does not detract from the liquid form of the solution itself, and potentially adds to the ionic conductivity through its ionic nature by also helping to dissociate the electrolyte ions. The one drawback in using ionic liquids is that they can quickly increase the viscosity of the solution. We therefore turned to ethyl methyl carbonate (EMC), an organic solvent commonly used in electrolyte solutions for lithium metal and lithium ion electrolytes to lower the overall viscosity of the solution. Figures 14, 15 and 16 show the results of the various iterations that used these cosolvents in combination with γ-BL as the base solvent.

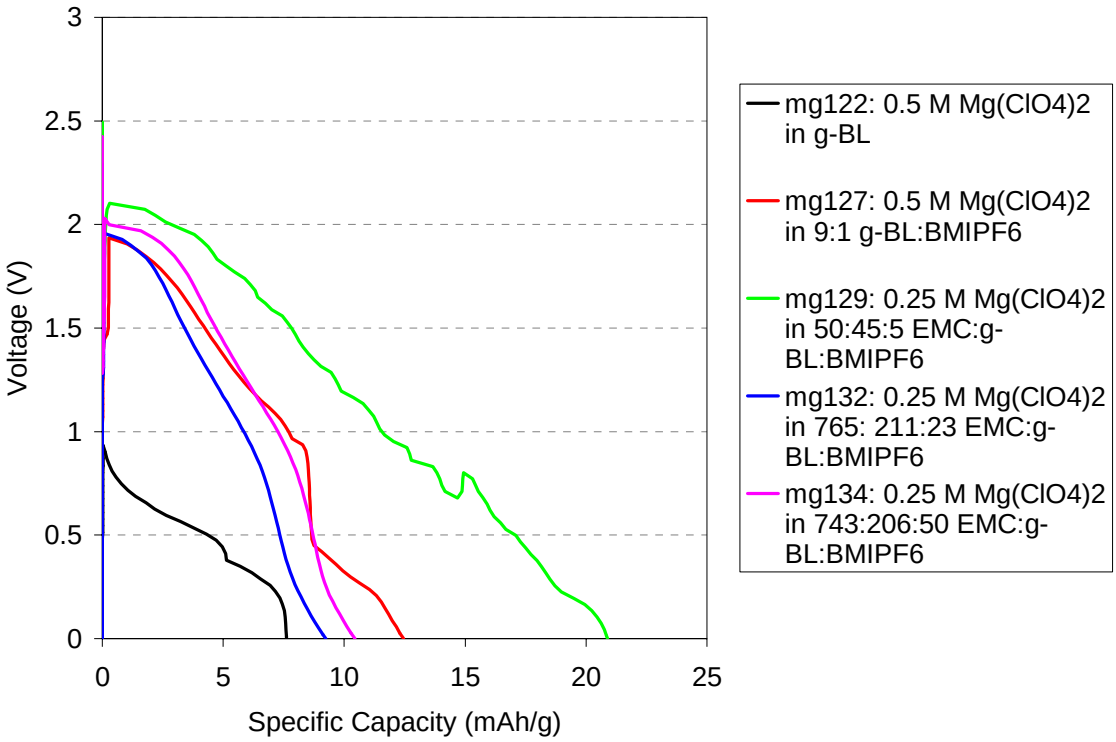

Figure 14: Full Discharge Profiles of AZ13B/λ-MnO_2 Cells with $Mg(ClO_4)_2$ in EMC:γ-BL:$BMIPF_6$ Electrolyte Solutions

Figure 14 shows the voltage curves for cells built based on Formula [3] in the fixtures shown in Figure 3(b). The λ-MnO_2 electrodes are PVdF-HFP bound. The base electrolyte solution delivers in this configuration only a small specific capacity at less than 1 V versus the

magnesium alloy. By adding just $BMIPF_6$ as 10% of the solvent mixture, not only does the capacity increase by 50%, but the overall voltage doubles, tripling the overall energy delivered by the cell. Decreasing the viscosity of this formulation by adding EMC and lowering the salt concentration to 0.25 M further increases both capacity and voltage. Further increasing the EMC concentration has a negative effect on capacity and voltage that is only slightly improved by increasing the $BMIPF_6$ concentration back to 5%.

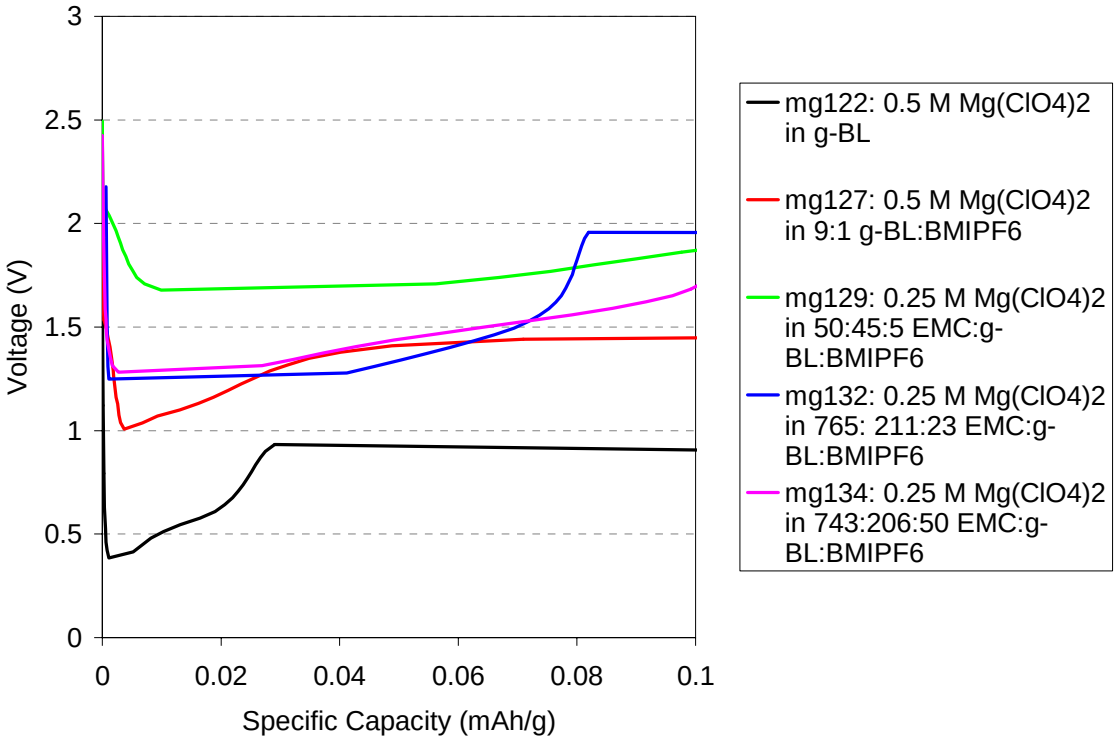

Figure 15: Initial Discharge Profiles of AZ13B/λ-MnO_2 Cells with $Mg(ClO_4)_2$ in EMC:γ-BL:$BMIPF_6$ Electrolyte Solutions

Figure 15 shows the voltage profiles of these cells upon initial discharge. The base electrolyte drops below 0.5 V initially and then recovers to near 1 V. In other words, the initial power output of the cell is half of the highest output of the cell, probably because the passive layer on the magnesium must be overcome for normal functioning of the cell. By adding the $BMIPF_6$, this voltage loss is much less compared to the overall potential of the cell. By lowering the viscosity of the cell by using a 50% EMC solution, the cell potential stayed above 1.5 V. More EMC seems to have a negative effect on this initial voltage, bringing it back to the level seen for the γ-BL/$BMIPF_6$ solvent mixture. Increasing the $BMIPF_6$ concentration does little to improve the situation.

In analyzing these results, we have weighed conductivity against other factors contributing to performance. Figure 16 shows the conductivity of each of these solutions over a range of temperatures. Of the five solutions presented here, the 9:1 solution is the most conductive at room temperature. However, this candidate is not the best performer in an actual cell. The high viscosity of the 9:1 solution seems to be making the diffusivity of the ions in solution the rate

limiting step. By lowering the viscosity with a low dielectric fluid such as EMC, we lower the conductivity, but allow for better flow. We see this effect in the better performing 50:45:5 solution, which has a lower overall conductivity than the 9:1 solution at temperatures above 0°C, but performs better in the actual cell than the 9:1 solution. Viscosity and conductivity must be balanced in this case. We observe with a 50% increase in EMC concentration a tremendous decrease in overall conductivity. This lack of conductivity is what is contributing to the lesser performance of cells using these electrolytes as compared to the 50:45:5 solution. All of these solutions still perform better than the base solution of 0.5 M $Mg(CLO_4)_2$ in γ-BL, indicating the importance of having a corrosive cosolvent such as the $BMIPF_6$ in solution.

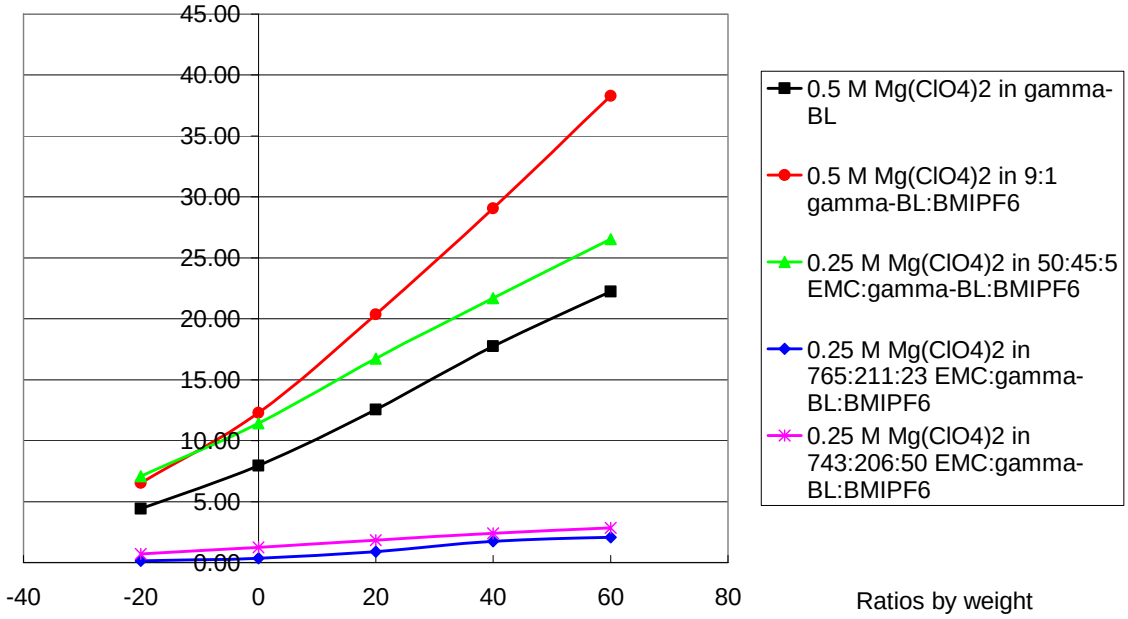

Figure 16

Figure 16: Conductivities of $Mg(ClO_4)_2$ in EMC:γ-BL:$BMIPF_6$ Electrolyte Solutions at Various Temperatures

However, the use of γ-BL and EMC have led to an optimization process in which conductivity due to dielectric and conductivity due to viscosity are in opposition. In order to bypass this optimization dilemma, the γ-BL and the EMC were replaced with AN. AN has a dielectric constant similar to that of γ-BL, but has a viscosity lower than EMC. By using AN, we should be able to see the limits of the $Mg(ClO_4)_2$ system in the closed cell.

Figure 17 compares the results of three cells. The first cell uses an electrolyte that contains only γ-BL and the salt. This cell barely discharges at all. Both capacity and voltage are extremely low. When EMC and $BMIPF_6$ are added to the solution, the cell voltage and capacity both improve greatly. Both are nearly double of γ-BL alone. By replacing the γ-BL and EMC with AN and increasing the concentration of $BMIPF_6$, the cell improves further. The discharge voltage increases beyond 2V to nearly 2.5V initially and the capacity is higher than the cell with the ternary solvent mixture. The parallel nature of these two lines seems to indicate that the mechanism of the reaction remains the same, but that the overall resistance has changed. With this combination, we seem to be approaching the upper voltage limit of the Mg/MnO_2 system.

Without a change in reaction mechanism, this system will probably not produce much more than what is shown in Figure 17.

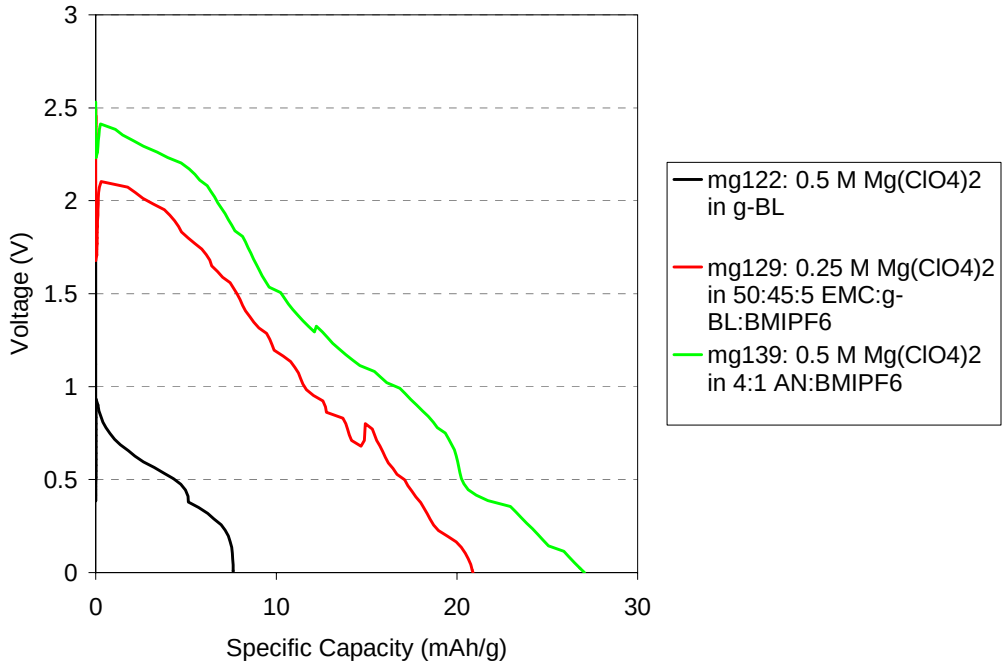

Figure 17: Comparison of Discharge of Mg/λ-MnO_2 Cells Containing the Baseline γ-BL with Cells Containing Assisting Solvents

$MgCl_2$. Magnesium chloride is an electrolyte that we looked into for several reasons. First, $MgCl_2$ is more environmentally benign than magnesium perchlorate. It is a more stable compound with its main decomposition products being HCl and magnesium oxide. Second, because it is more stable, it also has a lower safety risk involved in its use. Finally, the material we have in house is 98% pure, where the other two percent are water. This purity would facilitate a trace amount of water in each electrolyte, thus allowing for the water mechanism to take place in the cell without producing large amounts of gas. As we will discuss in later sections, water content can have a large beneficial effect on the capacity of the electrochemical cell. We use AN as the solvent for all of these solutions because of the promising results we saw with $Mg(ClO_4)_2$.

We began by looking at the effect of salt concentration on the solution. Using this 8:1:1 DMSO:AN:$BMIPF_6$ solvent mixture as our baseline mixture, we also took a look at electrolyte concentration effects on cell performance. The saturated 8:1:1 solution is compared to 0.25 M and 0.125 M concentrations of $MgCl_2$ in Figure 18. The 0.25 M solution is nearly saturated, which is why the upper portion of its discharge curve overlaps with the curve of the saturated solution. Some passivation effects at the anode due to inconsistent cleaning may be causing the deviation in these curves at lower voltages. These effects will be discussed later. The 0.125 M solution has improved discharge characteristics which are a result of overall better ionic mobility in solution.

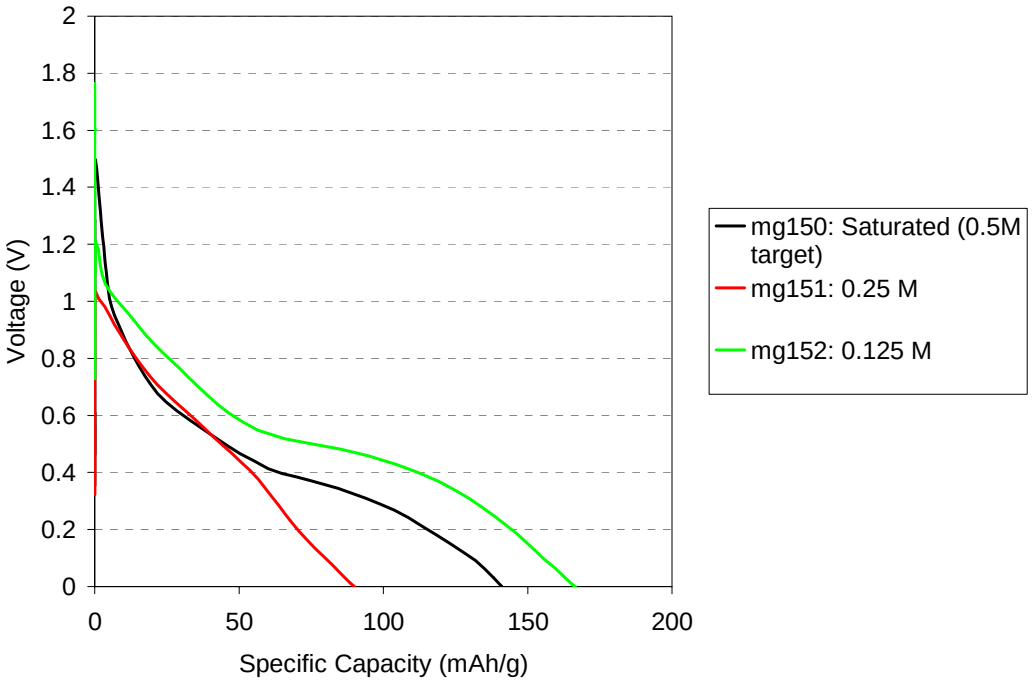

Figure 18: Molarity Effect of $MgCl_2$ on Discharge

The main concern with $MgCl_2$ is its solubility in the organic solutions. In many solvents, it reaches saturation quickly, at which point, ionic mobility is hindered, making the cells that use these electrolytes less effective. For this material, a solvent that helps enable solubility is needed to allow for better ionic mobility. We have used DMSO as just such a solvent.

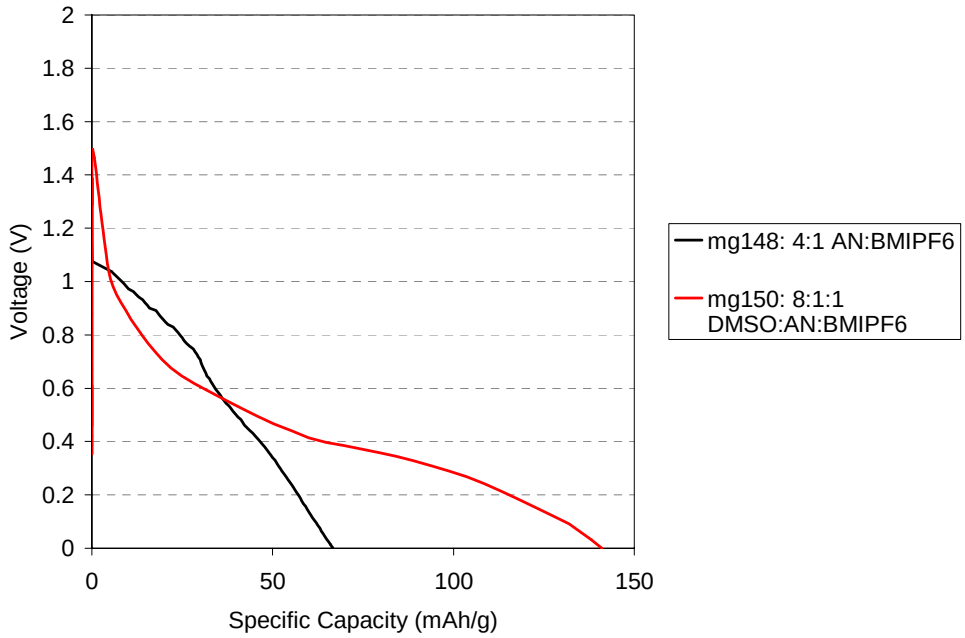

Figure 19: Effect of DMSO on Cells Containing $MgCl_2$ Electrolyte

Figure 19 shows the effect of DMSO on electrolyte solutions in cells based on Formula [3]. The target molarity in both cases is 0.5 M $MgCl_2$. In both cases, the solution is saturated. The solution containing the DMSO has solvated more of the $MgCl_2$. The capacity of the cell containing this solution has also improved substantially to where, if the voltage were not so low for most of the discharge, it would be an acceptable cell. The general shape of the discharge curve for these cells seems to indicate that the reaction mechanisms are different. In fact, for the cells containing DMSO, we tend to see a great deal of dark material migrating towards the anode, indicating the reaction involves the breakdown of the cathode material itself, as might be expected in the aqueous system.

The effect of $BMIPF_6$ on solutions containing $MgCl_2$ as a salt is also quite pronounced. The corrosive effect along with the dissociation of the Mg^{2+} and Cl^- ions causes a rather large increase in capacity, as seen in Figure 20. In this figure we observe a large increase in specific capacity just by modifying the 0.125M $MgCl_2$ solution to add $BMIPF_6$.

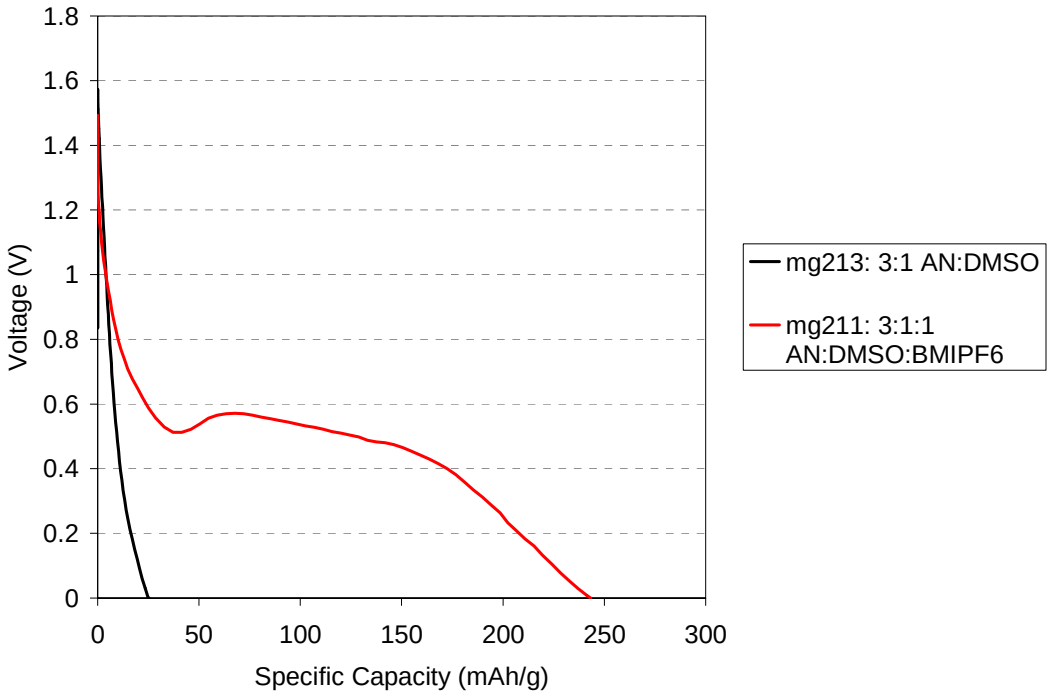

Figure 20: Comparison of Cells with Varying AN:DMSO:$BMIPF_6$ Ratios at a 0.125 M $MgCl_2$ Molarity

This increase in capacity seems in this case to be more related to the dissociation of the electrolyte ions as supported by the conductivity data shown in Figure 21. However, as was the case with the $Mg(ClO_4)_2$ solutions, a concentration limit exists for the $BMIPF_6$ in these types of solutions. At 30% $BMIPF_6$ concentration, the conductivity is lower than the solution at 20% $BMIPF_6$. This lower conductivity is most likely related to the increase in viscosity experienced in adding more $BMIPF_6$. In any case both electrolytes are similar in conductivity or better than the best electrolytes produced from $Mg(ClO_4)_2$.

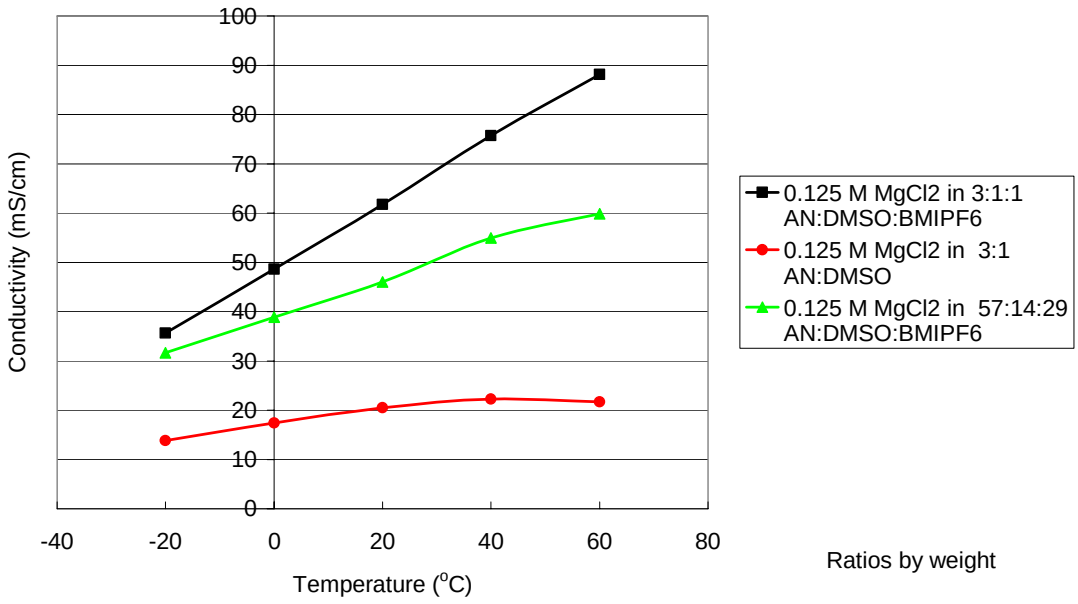

Figure 21: Conductivity Comparison of Electrolyte Solutions Containing $MgCl_2$

Figure 22 shows the results of cells that were produced using these optimized electrolytes. One of these cells has already been shown in Figure 20. Both cells demonstrate good capacity, with the 29% solution showing improved capacity, which seems contrary to the conductivity data. At these conductivity levels, the electrolyte solution is not the limiting factor in the cell. In this case it is probably the metal-solution interface itself. This interface is more readily removed in higher concentrations of $BMIPF_6$, thus leading to more activity from the cell.

Figure 23, on the other hand, shows more of an electrolyte effect. This figure is an expansion of the first seconds of discharge. In this time, the cell experience a capacitive effect surface experience a charge and the electrolyte ions move to compensate and neutralize this charge. The rate at which these ions can align and form a fully charged "capacitor" within the cell determines how long this voltage depression lasts and how severe it is. This voltage depression is detrimental to the functioning of fast acting electronic fuses and is best kept at a minimum. In the case of these two electrolytes, the higher viscosity solution causes a drop in voltage, while the lower viscosity electrolyte demonstrates almost no drop in voltage. Combining the information in Figures 22 and 23, we see that one electrolyte solution is more useful as a long term device while the other has the potential to be used in an "electronic fuse".

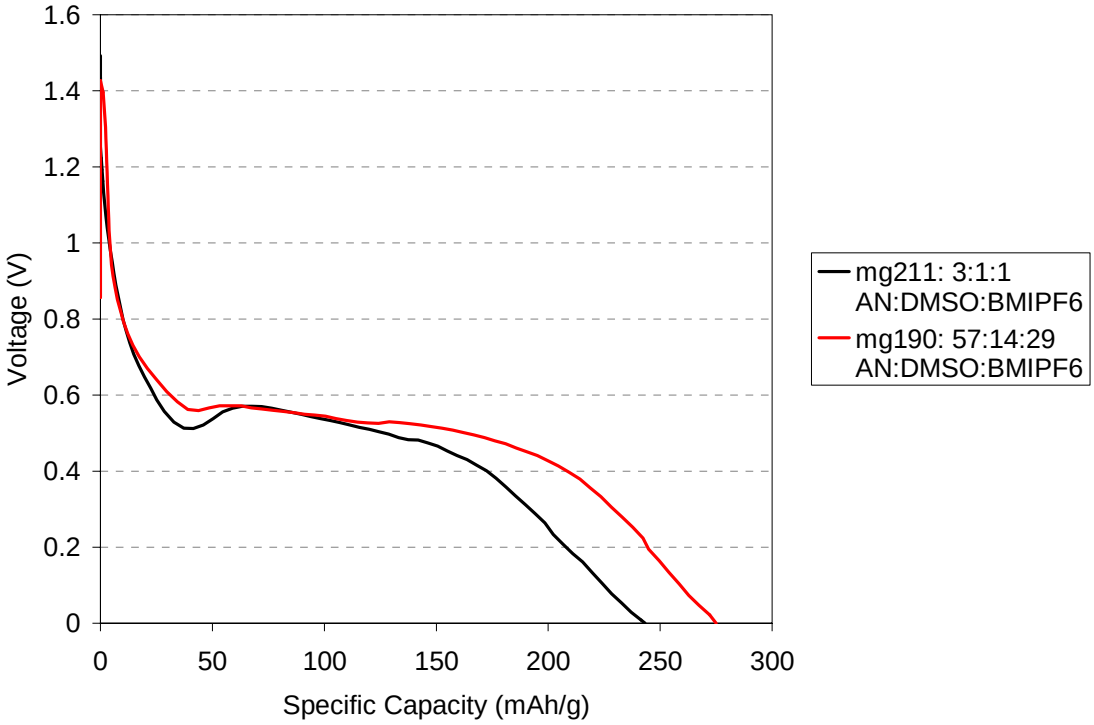

Figure 22: 0.1 mA/cm^2 Discharge Voltage Profiles of AZ31B/λ-MnO_2 Cells with Optimized Electrolyte Solutions

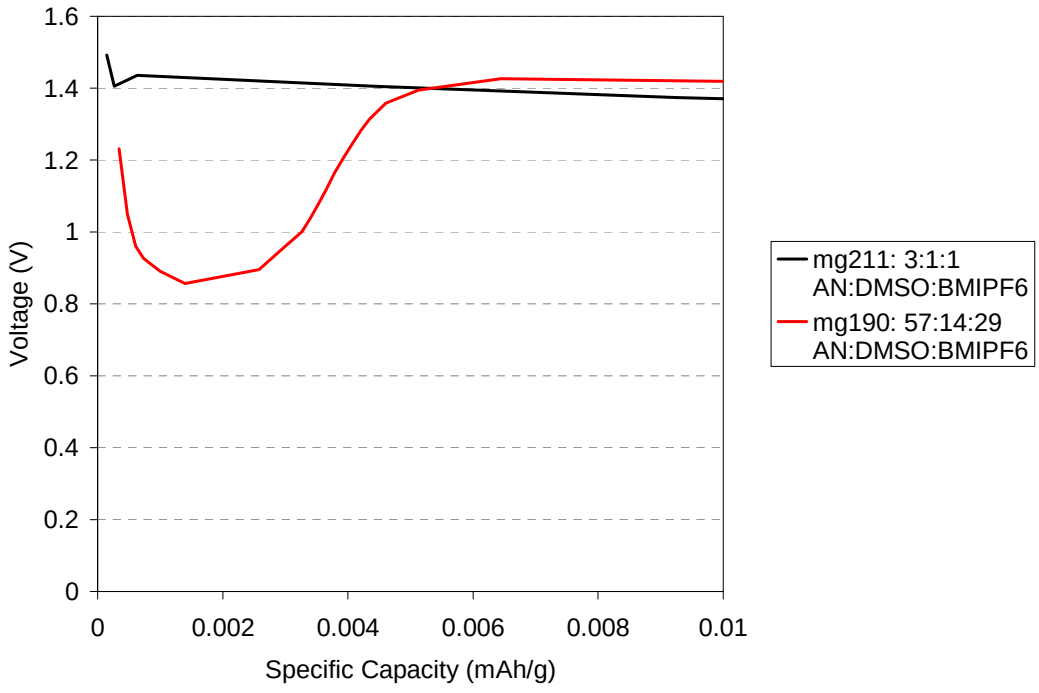

Figure 23: Same Cells as Figure 22 at the Initial Stages of Discharge

$\underline{Mg(SO_3CF_3)_2}$. Magnesium trifluoromethanesulfonate or magnesium triflate is the final of the three electrolytes tested at MaxPower. The physical properties of this substance are less well known, so it is difficult to determine whether it is an environmentally more friendly substitute for the perchlorate salt. The combustion products would presumably be HF, CO_2, SO_2, MgO and derivatives thereof. Several of these compounds do place a specific burden on the environment, which will have to be considered in the cell's destruction.

Cursory initial testing of this electrolyte was performed in the bagged cells described above to see its potential benefits. Figure 24 shows the results of this testing. In two of the three cases, an ionic liquid with matching anion was selected to help facilitate the dissolving of the electrolyte as well as provide an added corrosive material in solution to help break down the passive oxide layer on the anode. This ionic liquid is 1-butyl-3-methylimidozolium trifluoromethanesulfonate. The solutions were all measured to be 0.125 M. The AN:BMItrif solution was saturated, demonstrating the need to have DMSO in solution. In general these cells all performed worse than the $MgCl_2$ cells. They never discharged above 1 V and had generally poor specific capacities, as the figure shows. Because of these results, emphasis was not put on developing this system any further.

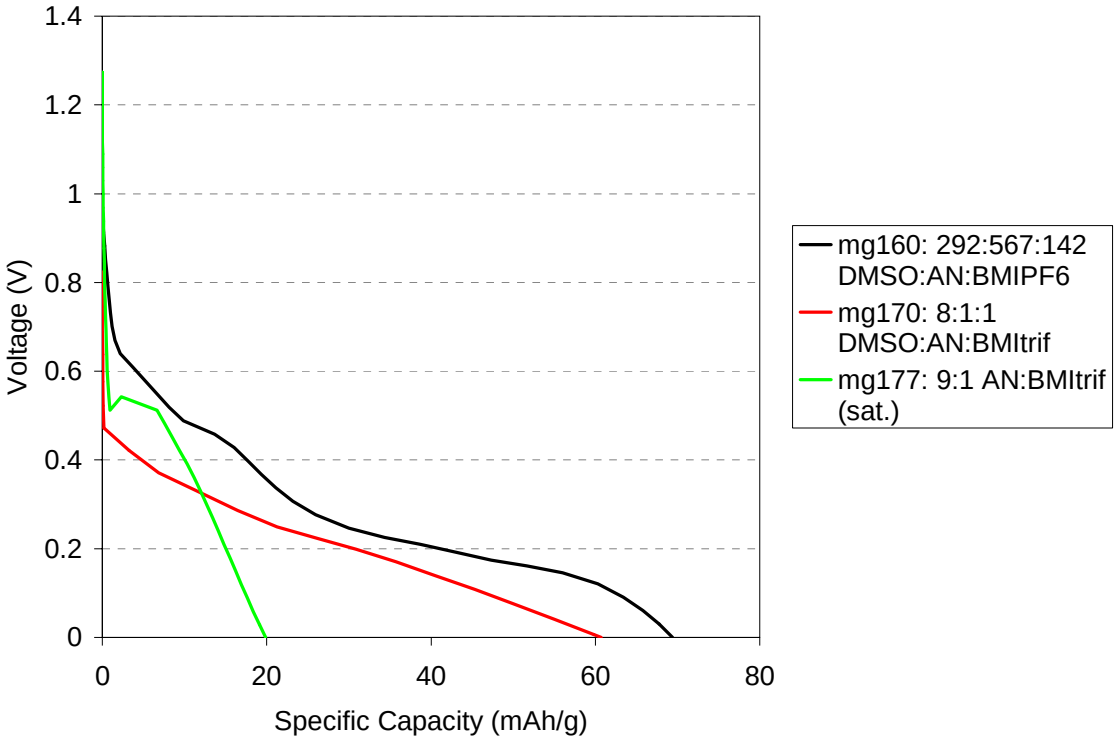

Figure 24: Discharge Comparison of Cells that use $Mg(CF_3SO_3)_2$ as an Electrolyte

2.2. Mg Half-Cell Studies

Oxide Removal. Passivation is an important aspect of this program. The passive oxide layer on the magnesium must be removed for the cell to function properly. We concentrated a good portion of the program on finding ways to break down the oxide layer chemically through

solution chemistry. For a good portion of this program, the anodes used in the bags were cleaned in the dry room, but not under argon for logistical reasons. We have recently been able to overcome these logistical problems and are now able to clean the anode and add electrolyte in the glove box. Several electrolyte solutions were tested twice, once after assembly under air and once after assembly under argon to examine the effect of the oxide layer on the magnesium anode including the two most promising ones. We found that the effect of removing the oxide layer and not allowing it to reform in air to be large.

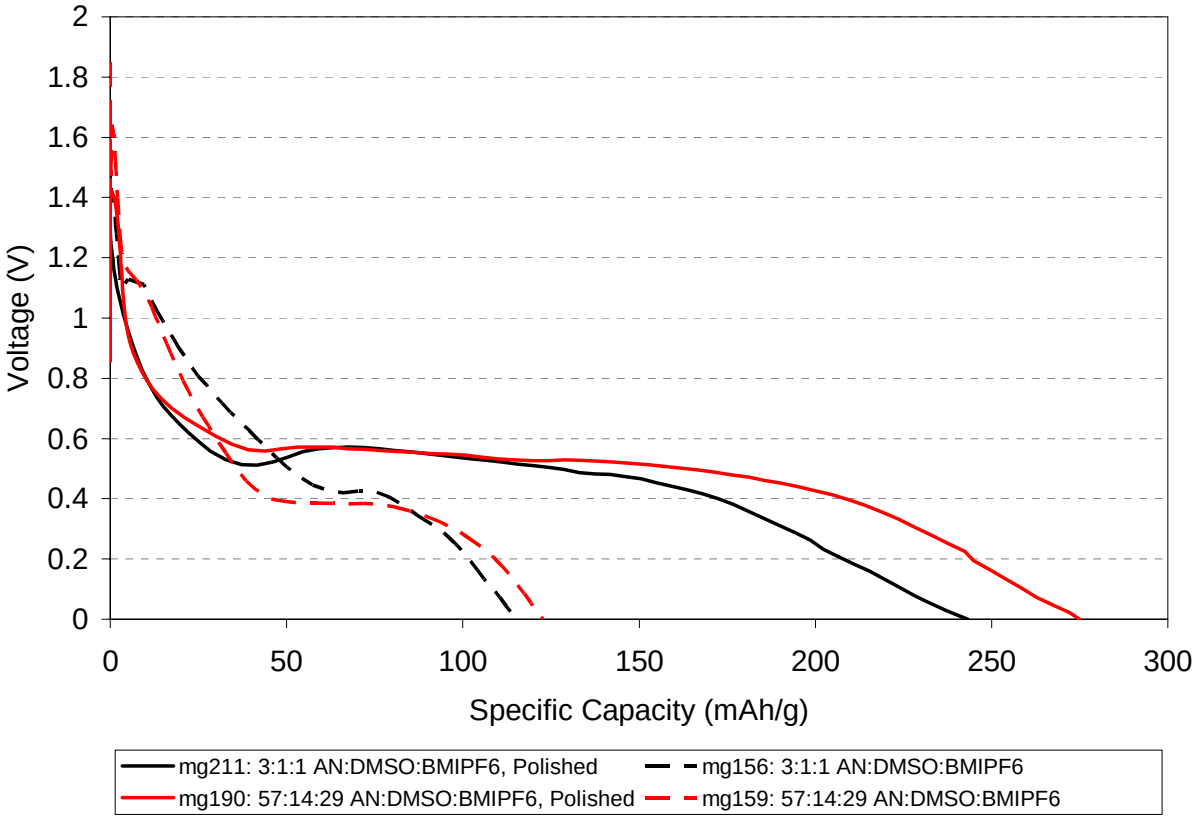

Figure 25: Discharge Comparison of Mg/λ-MnO_2 Cells with Oxide Layer Removal under Argon ("Polished") and without Oxide Layer Removal Containing 0.125 M $MgCl_2$ in Three Varying Solvent Mixtures

Figure 25 shows the two most promising electrolyte solvent mixtures tested from assembly under air and assembly under argon (polished). The legend for this figure shows the ratio of AN to DMSO to $BMIPF_6$. Each electrolyte has a molarity of 0.125 M. This figure shows the importance of having an oxide free surface on the anode. In air, even if cleaned and polished, the oxide film reforms too quickly to achieve optimum results. Under argon the oxides do not form on the metal surface after it has been cleaned. Since the oxide passivates the surface of the anode, this oxide covered surface does not participate in the electrochemical cell, thus causing the loss in capacity seen in Figure 25.

The effect of polishing is not limited to solutions containing $MgCl_2$. Figure 26 shows the results of a similar test on $Mg(SO_3CF_3)_2$. The polished electrode also showed definite capacity

improvement with this polishing. This fact demonstrates that the improvement is a function of the anode and that it is still a necessary step in the assembly of these cells.

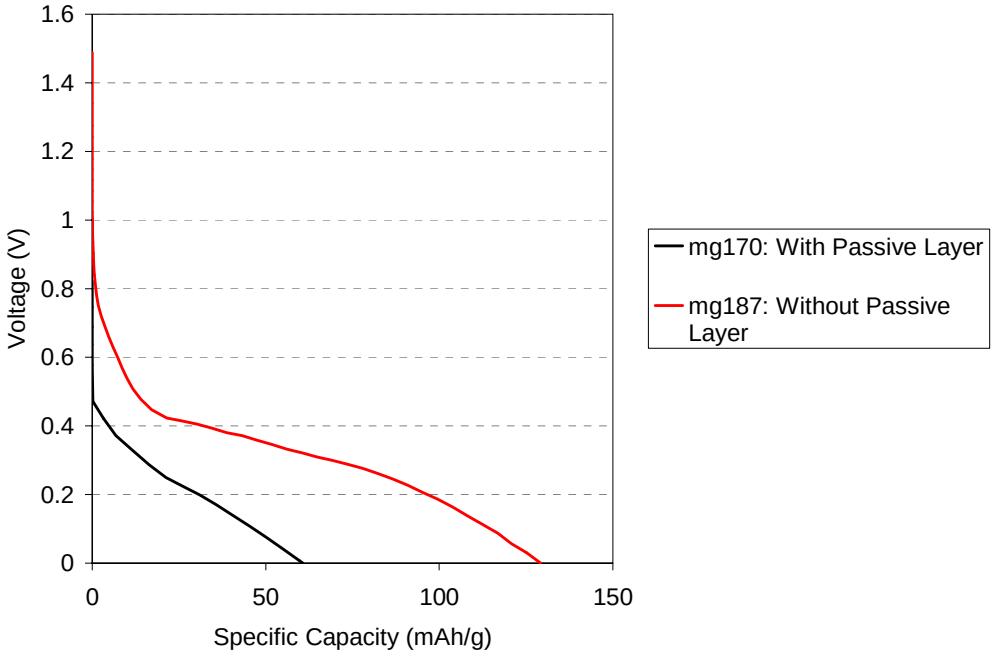

Figure 26: Effect of Oxide Layer Removal in Cells Containing Mg Triflate Electrolyte

Alloys. In addition to removing the passive layer, we have looked into other alloys and ceramics that might potentially have less of a passive layer or a more readily removed passive layer. The materials studied were magnesium metal, AZ31B, Mg2Si and MgxC.

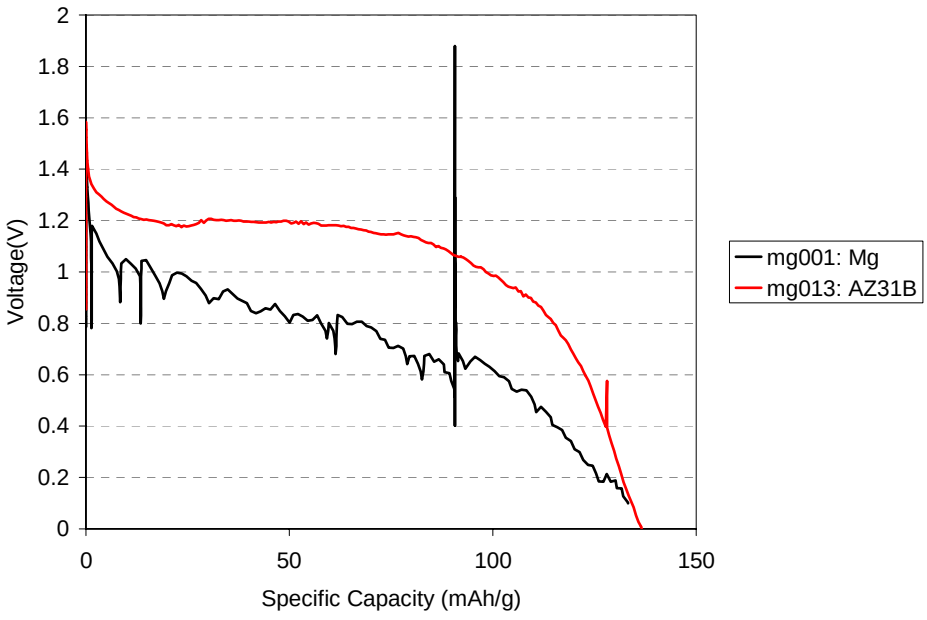

Figure 27: Comparison of Discharge Voltage Profiles of Mg Metal and AZ31B Alloy

Magnesium metal and AZ31B were studied initially as potential baseline materials because of their high magnesium content. Magnesium metal comes in several forms, but is presently in its purest for expensive. AZ31B is less expensive and is also available in several forms, including metal sheets. AZ31B has also been used extensively in aqueous magnesium batteries, which makes it an interesting candidate for the present non-aqueous cells.

Figure 27 shows the discharge curves of magnesium rod and AZ31B versus λ-MnO2 in 0.5 M Mg(ClO4)2 in PC. Both of these cells were tested in the fixture shown in Figure 3(a). We observe drops in potential followed by quick recoveries in the magnesium metal cell. This behavior is probably a result of local passivation on the metal followed by some removal of the passive layer. The AZ31B material exhibits little or none of this behavior. The 3% aluminum and 1% zinc may be preventing the formation of surface oxides, allowing the reaction to occur more efficiently. For this reason, the AZ31B material was used most extensively as an anode.

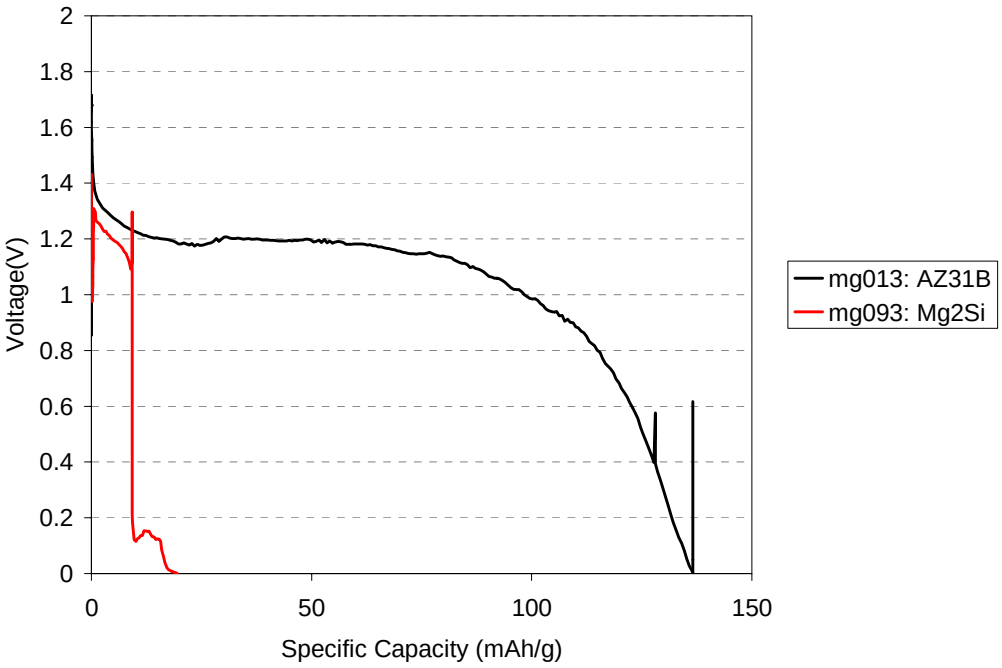

Figure 28: Comparison of Discharge Voltage Profiles of AZ31B Alloy and Mg_2Si Powder versus λ-MnO_2

We also looked into using Mg_2Si as an anode mainly because it is a ceramic powder which would both offer more surface area and possibly even bind the Mg strongly enough that the oxide layer would not form. When compared to this anode, AZ31B still is still the superior anode. Figures 28 and 29 show AZ31B compared to Mg_2Si in two different cells. Figure 28 is an anode material/λ-MnO_2 cell in the fixture shown in Figure 3(a), while Figure 29 is an anode material/MoO_3 cell built and sealed under argon in an aluminum lined bag. In both cases, the Mg_2Si can only manage a small fraction of the capacity of the AZ31B. Apparently, either the oxide layer is still forming, or the ceramic matrix does not readily release the magnesium ions.

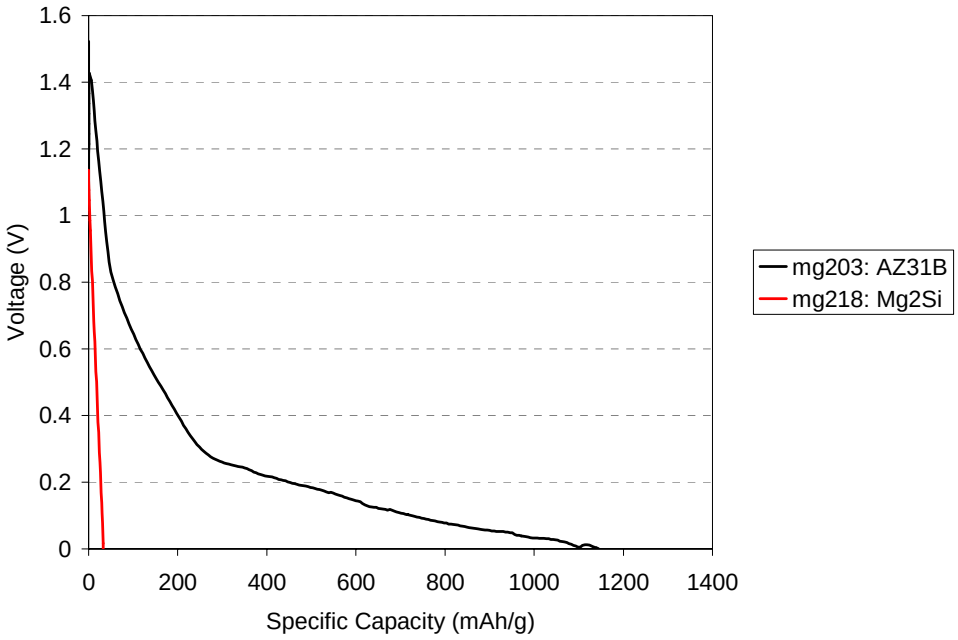

Figure 29: Comparison of Discharge Voltage Profiles of AZ31B Alloy and Mg_2Si Powder versus MoO_3

Since the extraction of the Mg from Mg_2Si was a possible cause of its poor performance, we explored the possibility of depositing Mg into a graphitic matrix. We looked at different deposition levels from dopant levels to the amount expected based in lithium intercalation. This deposition was done as described in the Materials and Methods section above. The XRD results of this work are shown in Figure 30.

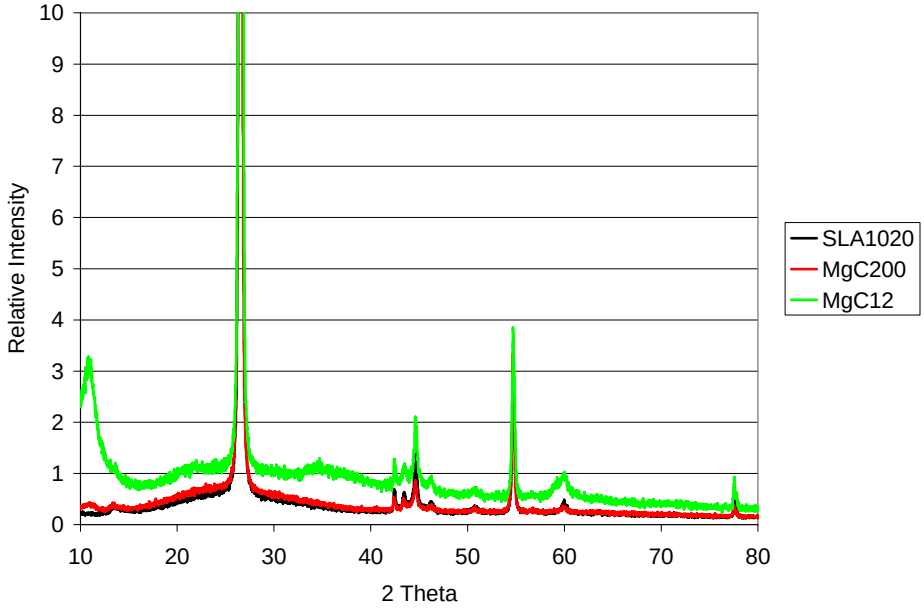

Figure 30: XRD Spectrum of Carbon with Increasing Mg Doping

Figure 30 is an expansion along the relative intensity axis of the XRD scan. The carbon peak at 28° would dominate this spectrum otherwise. In this case, the carbon lattice seems to be retained along with all of its parameters. The only change when the magnesium is added is that the carbon gains a slightly more amorphous nature. At these levels the magnesium would be difficult to detect.

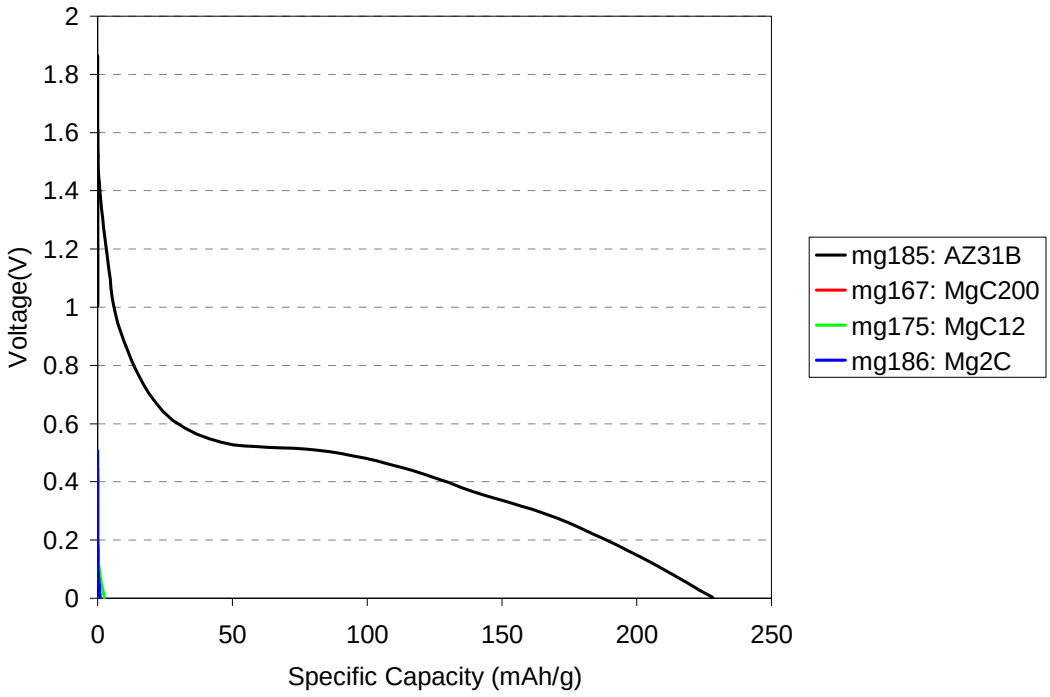

Figure 31 Comparison of Discharge Voltage Profiles of AZ31B Alloy and Mg_xC Powder versus λ-MnO_2

Figure 31 shows the discharge curves of these materials and AZ31B in aluminized bags versus λ-MnO_2. In all cases, including a later analogue to the Mg_2Si material, the capacity of these cells is poor. As with lithiated carbon, magnesiated carbon is probably not stable in air and tends to for the oxide. Since the particles are dispersed and in powder form in this case, the oxide completely removes the magnesium from the reaction. Unfortunately, the facilities needed to manufacture these materials in an inert atmosphere would be prohibitive in cost. This material was, therefore, not explored any further.

Mg/Cathode Studies

Competing Reactions. When devising this program, we were interested mostly in the insertion of magnesium into λ-MnO_2 because of the high voltage, and, therefore, high energy, cell that the system would produce. In several of our studies, we have seen the formation of $MgMn_2O_4$ as shown in the XRD spectrum in Figure 32. This spectrum compares the pristine λ-MnO_2 material and the material after being discharged in a magnesium cell. In the post-discharge spectrum a

new peak appears and actually dominates the spectrum. This peak and its spectrum are consistent with the spectrum for $MgMn_2O_4$.[8]

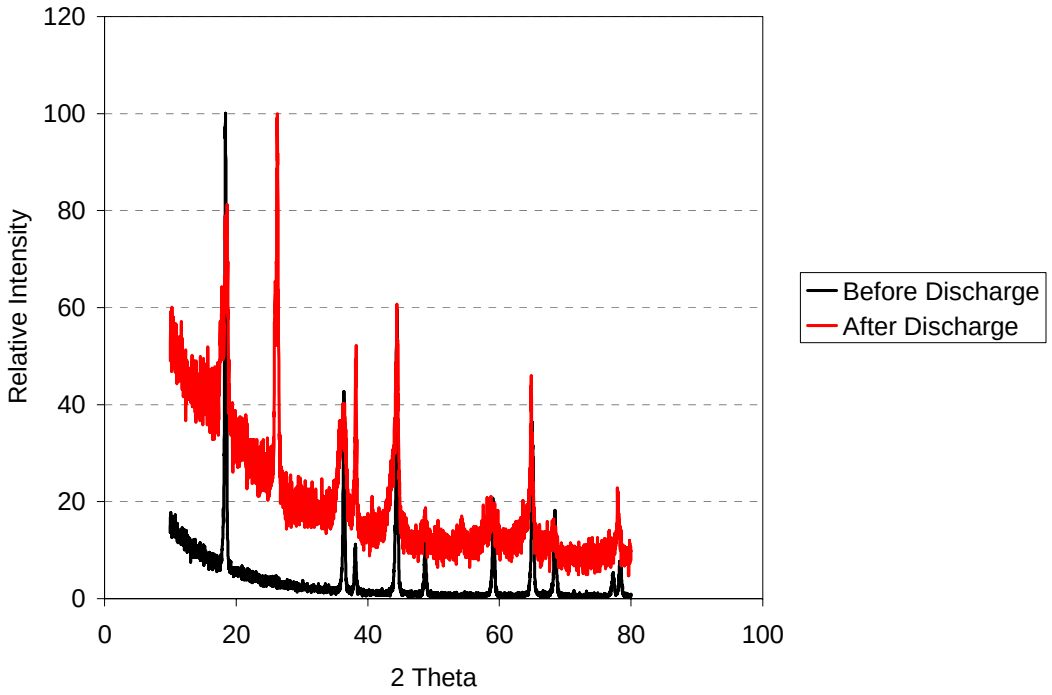

Figure 32: XRD Spectra of λ-MnO_2 Before and After Being Used in a Magnesium Cell

Although this reaction was desired, it is not always the only one seen in this system. The aqueous reaction is also in competition and may indeed help to partially assist in the intercalation if present in small amounts. Figure 33 shows the overall discharge profile for the Mg/λ-MnO_2 system. This profile demonstrates the Mg/λ-MnO_2 cell in an open atmosphere in 0.5M $Mg(ClO_4)_2$ electrolyte, whose voltage averages 1.2 V for this electrolyte solution for 140 mAh/g. This cell was discharged in the fixture shown in Figure 3(a), which is partially open to the atmosphere. In this case oxygen can get into the solution and form hydroxide ions at the cathode current collector or water can be absorbed and converted to hydroxide by the cathode itself. Meanwhile, the hydroxide reacts with the anode to draw the magnesium into solution. If too much water is used, another side reaction can occur, resulting in the production of hydrogen. All of these reactions can be summarized by Formulae [4-7].[9]

$Mg + 2OH^- \Rightarrow Mg(OH)_2 + 2e$	Aqueous Anode Reaction	[4]
$2MnO_2 + H_2O + 2e \Rightarrow Mn_2O_3 + 2OH^-$	Aqueous MnO_2 Reaction	[5]
$O_2 + 2H_2O + 4e \Rightarrow 4(OH)^-$	Aqueous O_2 Reaction	[6]
$Mg + H_2O \Rightarrow Mg(OH)_2 + H_2$	Aqueous Side Reaction	[7]

[8] N.K. Radhakrishnan, A.B. Biswas, *Z. Kristalloogr., Kristallgeom., Kristallphys., Krystallchem.*, **142** (1975) 117 (PDF File)
[9] David Linden, Thomas Reddy, Eds. *Handbook of Batteries, 3rd Ed.*, McGraw-Hill: New York, 2002

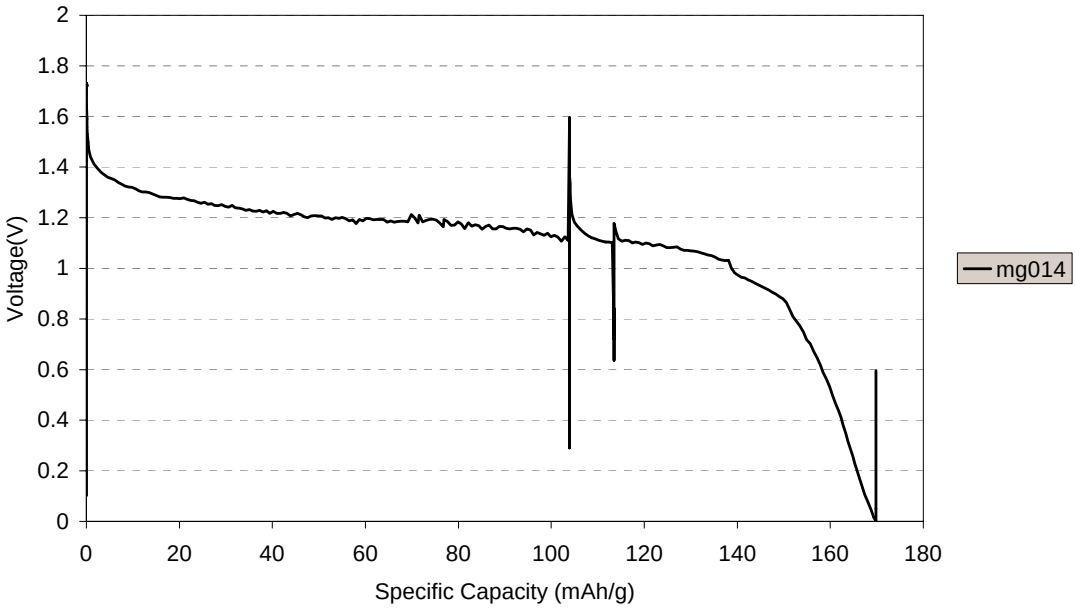

Figure 33: Low Rate Discharge of Mg/λ-MnO_2 Cell

The cells shown in Figure 34 are also discharged in the fixture shown in Figure 3 and contain 0.25 M Mg(ClO4)2 solution in the solvents listed in the legend. The overall capacity for these cells is large and the voltage is low. Gas formation can be seen in the fixture at the magnesium and manganese electrodes, and solids are formed after the reaction is complete. These cell reactions are almost all due to water, since they did not perform at all without water.

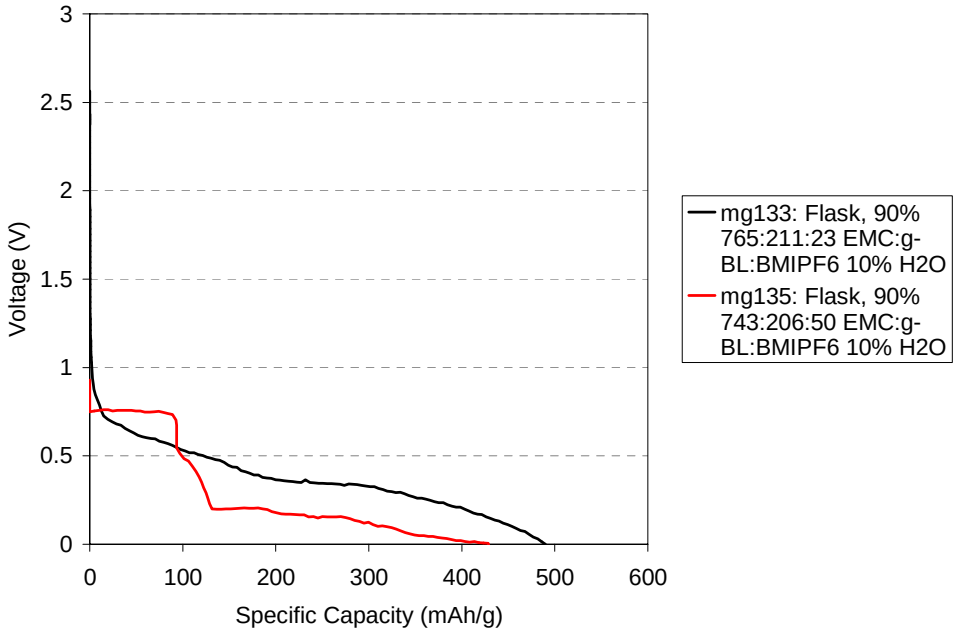

Figure 34: Discharge Profiles of AZ13B/λ-MnO2 Cells with $Mg(ClO_4)_2$ in EMC:γ-BL:$BMIPF_6$ Electrolyte Solutions with Water Additive

Although these cells are desirable from a capacity standpoint, they are less desirable from a voltage and safety standpoint and may not be applicable to "electronic fuse" applications. These results seem to suggest that a trace of water is beneficial, but too much is impractical and even dangerous. We therefore constrained ourselves to dry solvents and salts that contained small amounts of water, on the order of magnitude of 1% to 2% of the salt mass.

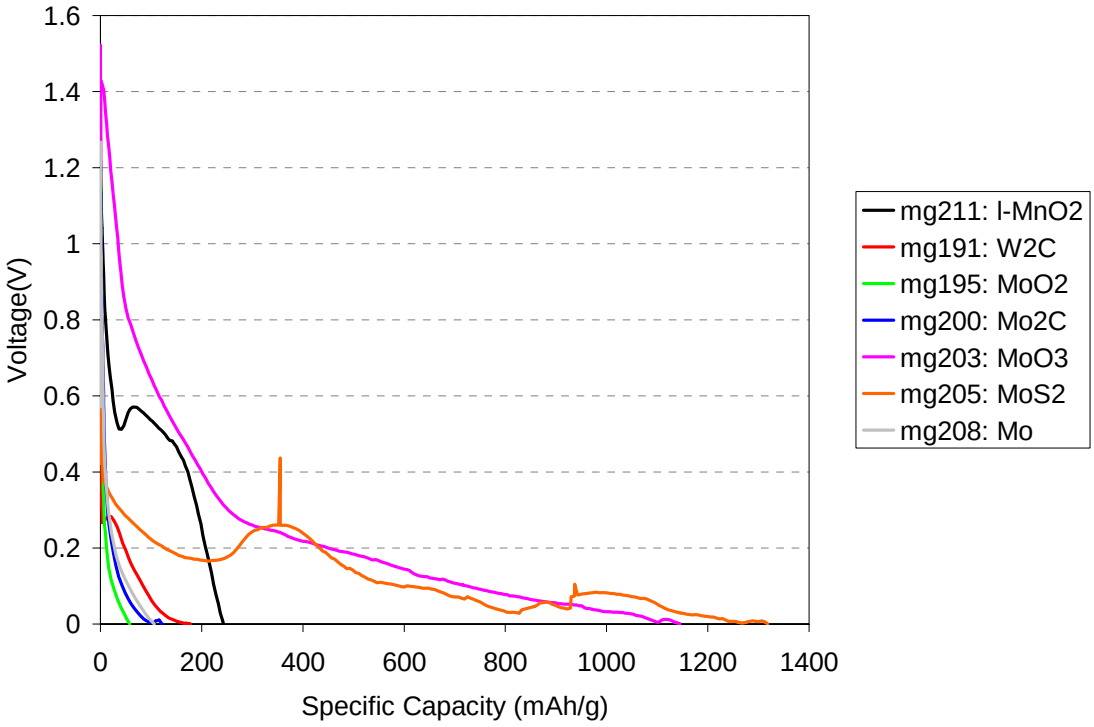

Figure 35: Comparison of Discharge Characteristic of Several Cathodes Versus AZ31B

Other Cathodes. Because the voltage of the MnO_2 candidate was not as high as expected except when exposed to the air and water, we began to explore several other possible alternative cathodes for this system. We looked at several candidates, most of which were molybdenum based. We looked at so many of this type of material because the trioxide compound and the sulfide compound gave us such promising results, as shown in Figure 35. Of all of these materials, from an energy standpoint, the MoO_3, λ-MnO_2 and MoS_2 material were the best by far. Despite its good capacity, the sulfide was not pursued further because its voltage was very low and as a sulfide, it might not be the best candidate environmentally.

We focused some effort on the MoO_3 to see what it could achieve as far as fuse applications were concerned and tested it under the $5mA/cm^2$ and $10mAh/cm^2$ conditions to see how it would perform. Initially, the cell dropped immediately to zero, but a second pulse did succeed in both cases, as is demonstrated by Figure 36. At these rates, we are able to get 0.4 V to 0.5 V out of these cells, which is 100% higher than their average voltage at 0.1 mA/cm^2. With some creative design, these cells might be viable candidates for certain fuse applications.

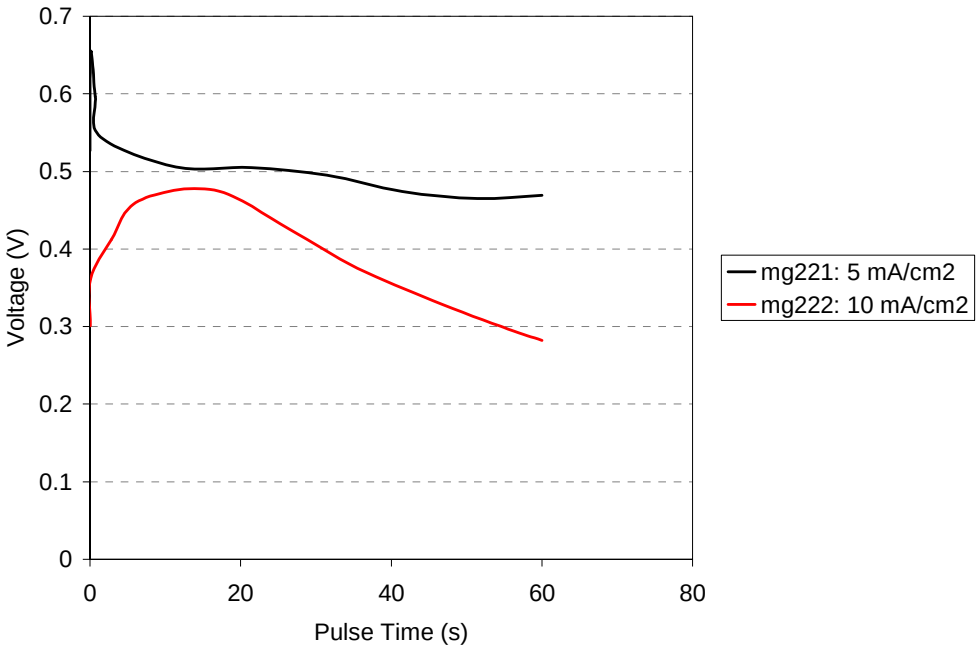

Figure 36: 60 Second Pulse Voltage Profiles for Mg/MoO_3 Cells

Lithium Ion Doping. Another method of overcoming some of the shortfalls of the magnesium system at least with respect to λ-MnO_2 is through doping the electrolyte with lithium ions. We found when doing initial testing of this system that a 0.1 M $LiPF_6$ concentration can have a great effect on the discharge of one of these cells

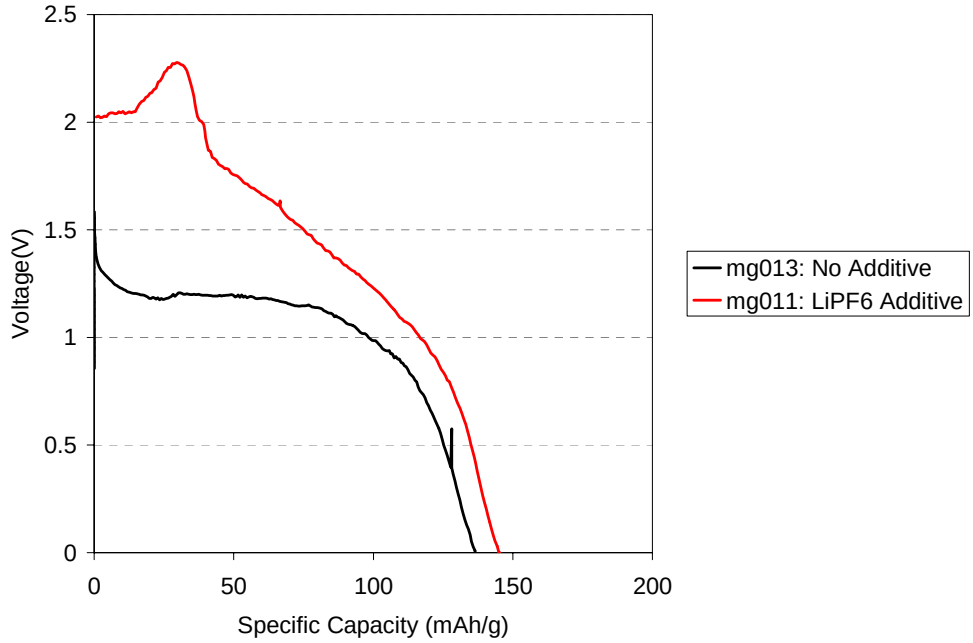

Figure 37: Effect of Li^+ Ions in Magnesium Electrolyte Solution on AZ31B/λ-MnO_2 Cells

Figure 37 shows the results of lithium ion doping in one of these cells. In the doped cell, instead of seeing a single plateau during the discharge, two are clearly visible. The first one is the insertion of lithium ions into the MnO_2 matrix to form $LiMn_2O_4$. The lithium ions are replaced by magnesium in solution and no gasses are formed through the reaction and no lithium metal is used in the cell. This system was not pursued because a hybrid lithium-magnesium system was not a part of the mandate of the project, but its advantages are clear. Even though it does not have the specific capacity of a MoO_3, but its voltage is five times greater giving it the advantage in certain short burst fuse applications and the potential to compete in terms of energy with an optimized electrolyte solution.

Conclusions

This research dealt with the question of developing a more environmentally benign, safe, cost effective electrochemical system for reserve battery applications. By employing magnesium as the anode, safety was addressed immediately. The selection of MoO_3 and MnO_2 as cathodes certainly makes this system a step up environmentally from the oxyhalide cathodes typically employed in such applications. These materials are also all relatively inexpensive.

The use of ionic liquids, and in particular, $BMIPF_6$ was a real breakthrough for the non-aqueous magnesium system. In electrolyte solutions containing these materials, three to tenfold energy improvement was observed over solutions that did not contain these materials. While they still cannot fully remove an air-formed oxide layer, they prevent the formation of an impervious layer by the electrolyte solvents and improve solution conductivity by aiding in the dissociation of the electrolyte salts. With these improvements, we estimate that the present best system using MoO_3 as the cathode would produce a D-size battery with 9.8 Wh of available energy.

Despite the progress seen through the implementation of ionic liquids in the electrolyte solution, the non-aqueous magnesium system still has certain limitations, the most prominent of which is the oxide layer which builds up quickly in open air. The magnesium metal still has to be polished under argon for its full potential to be realized. This step in a manufacturing process can be costly, and in a cell that is to sit on a shelf for years oxide free magnesium can be difficult to maintain. Any future work in this area would have to continue to address this problem.

For our part we would suggest three methods that would have to be explored to make this environmentally friendlier technology viable. First, we would suggest a further broadening of the experimentation on ionic liquids to encompass more candidates. Several of these materials are strong Lewis acids which can improve on the capability of the ionic liquids explored here in their ability to break down the metal oxide layer and dissociate the electrolyte. Second, we would suggest building upon our findings with the lithium/magnesium ion salt. These findings were extremely encouraging in that a small concentration of lithium ions in solution could bring out the high voltage plateau of the manganese oxide material. Further improvement of this system could produce a cell that is every bit as environmentally sound as the pure magnesium cell with a much higher energy density. Finally, we would suggest the identification of manufacturing equipment that would be able to handle inert electrode polishing. In the event that internal chemical means are not enough to overcome the magnesium oxide layer, a closer look at what it would take to manufacture these cells under inert anaerobic conditions would be warranted.

Appendices

Supporting Data

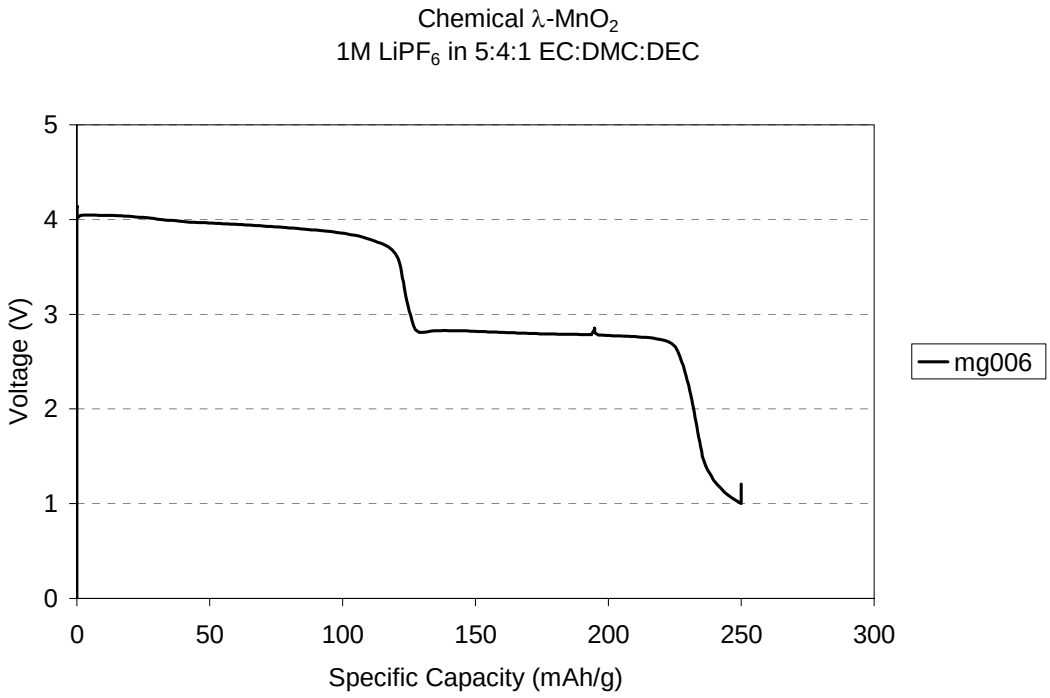

Typical Teflon λ-MnO_2 Cathode Discharge Versus Lithium

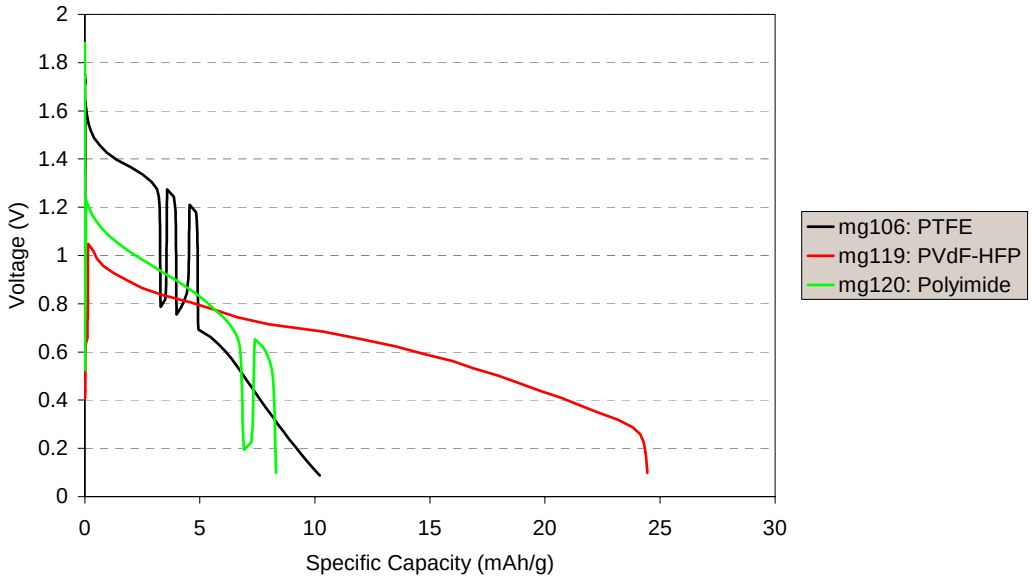

Low Rate Discharge of Mg/λ-MnO_2 Cell in Constrained Fixture Cell with 0.5 M $Mg(ClO_4)_2$ in PC

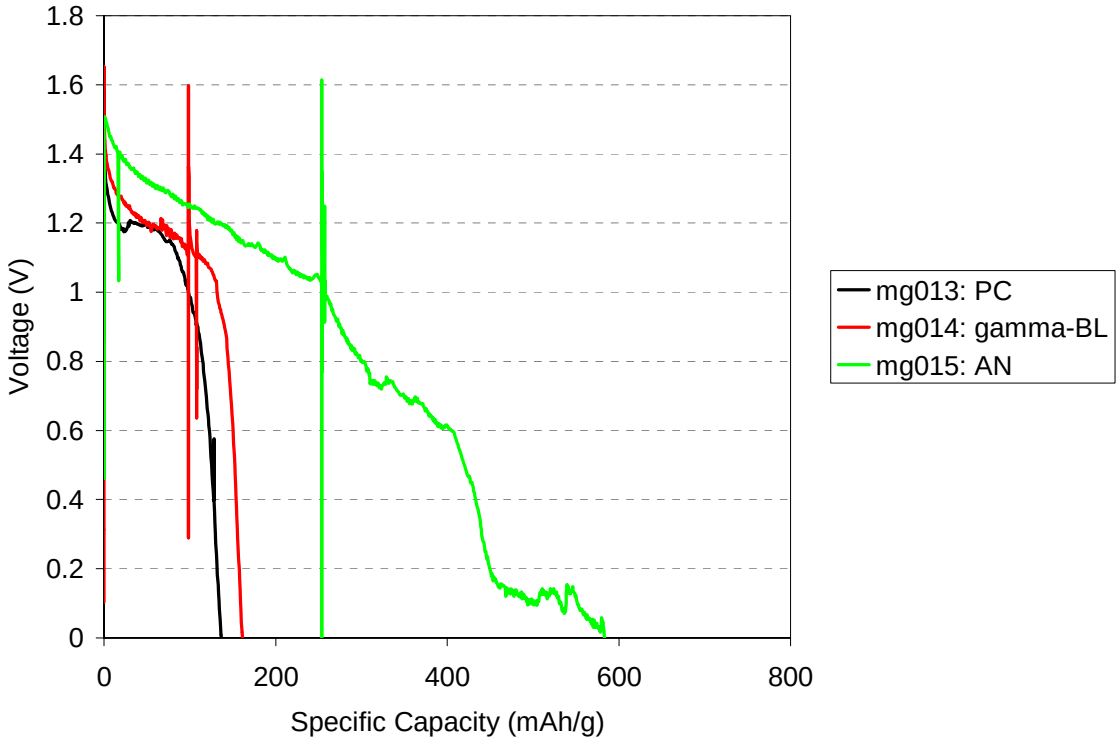

Discharge Profiles of Base Solvents with 0.5M $Mg(ClO_4)_2$ in AZ13B/λ-MnO_2 Cells

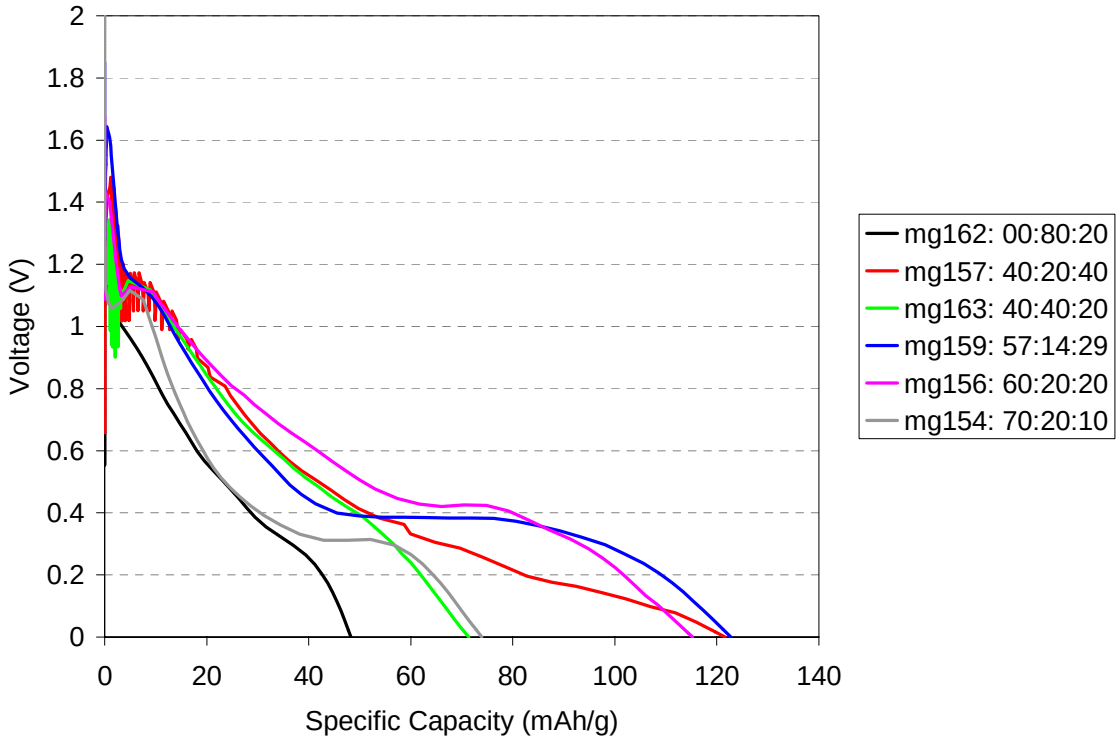

Comparison of Cells with Varying AN:DMSO:$BMIPF_6$ Ratios at a 0.125 M $MgCl_2$ Molarity

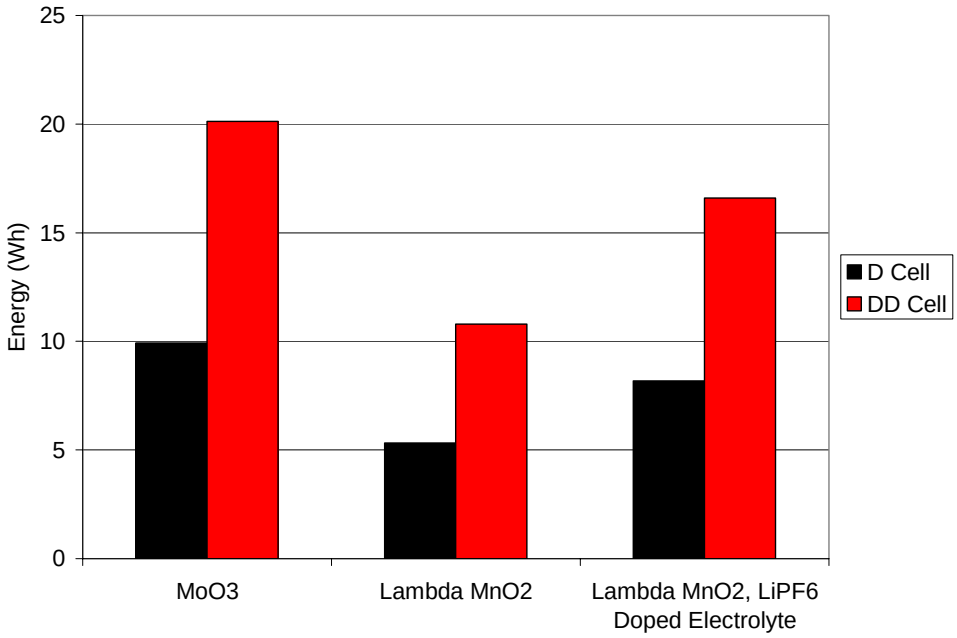

Energy Available in D and DD Size Batteries for Current Best Non-Aqueous Magnesium System

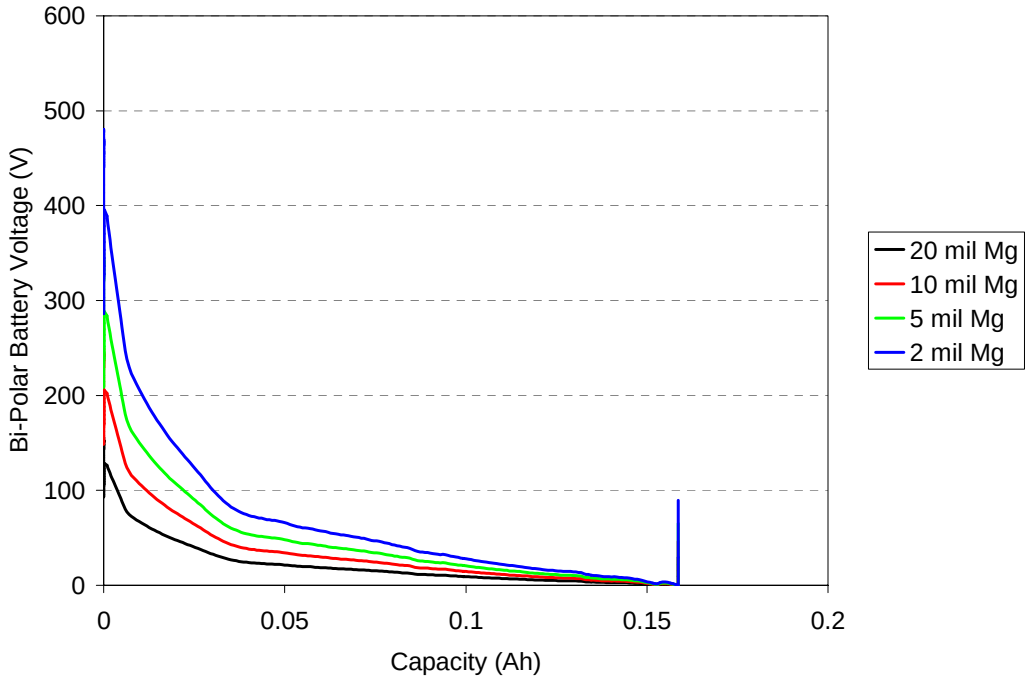

Projected Low Rate Discharge Profiles of D Size Bipolar (Series Only) Mg/MoO_3 Batteries at Various Mg Anode Thicknesses (1mil=25.4µm)

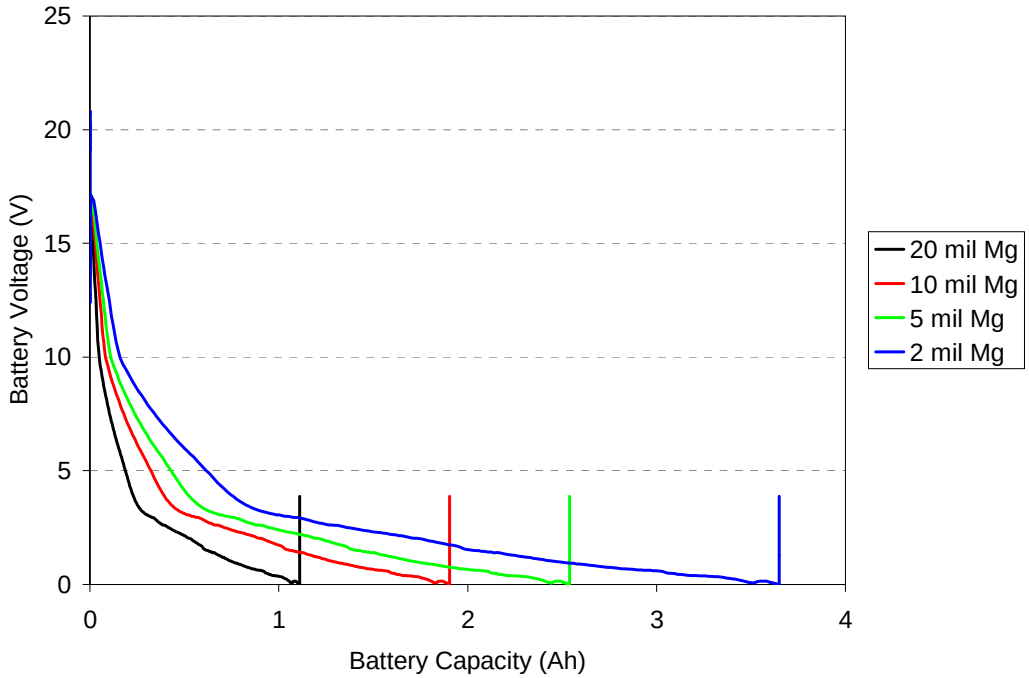

Projected Low Rate Discharge Profiles of D Size Bipolar (Series and Parallel) Mg/MoO_3 Batteries Set to a 12V Average Discharge Voltage at Various Mg Anode Thicknesses (1mil=25.4μm)

List of Technical Publications

Develop A Low Cost, Safe And Environmentally Benign High Energy And High Rate Reserve Battery, SEED Project Outbrief, In-Progress Review Meeting, March 17, 2004

Improvements in Magnesium Batteries through Ionic Liquids: A Step towards an Environmentally Benign Reserve Battery, "Partners in Environmental Technology Technical Symposium & Workshop", November 30 - December 2, 2004